DEPOSITIONAL FACIES AND AQUEOUS–SOLID GEOCHEMISTRY OF TRAVERTINE-DEPOSITING HOT SPRINGS (ANGEL TERRACE, MAMMOTH HOT SPRINGS, YELLOWSTONE NATIONAL PARK, U.S.A.)

BRUCE W. FOUKE,[1] JACK D. FARMER,[2]* DAVID J. DES MARAIS,[2] LISA PRATT,[3] NEIL C. STURCHIO,[4] PETER C. BURNS,[5] AND MYKELL K. DISCIPULO[2]

[1] *Department of Geology, University of Illinois, 245 Natural History Building, 1301 W. Green Street, Urbana, Illinois 61801, U.S.A. e-mail: fouke@iiiuc.edu*

[2] *Exobiology Brunch, MS 239-4, NASA Ames Research Center, Moffett Field, California 94035, U.S.A.*

[3] *Biogeochemicul Laboratories, Department of Geological Sciences, Indiana University, Bloomington, Indiana 47405, U.S.A.*

[4] *Environmentul Research Division. Argonne National Laboratory, 9700 South Cuss Avenue, Argonne, Illinois 60439. U.S.A.*

[5] *Department of Civil Engineering and Geological Sciences, University of Notre Dame, 156 Fitzpatrick Hull, Notre Dame. Indiana 46556, U.S.A.*

ABSTRACT: Petrographic and geochemical analyses of travertine-depositing hot springs at Angel Terrace, Mammoth Hot Springs, Yellowstone National Park, have been used to define five depositional facies along the spring drainage system. Spring waters are expelled in the vent facies at 71 to 73°C and precipitate mounded travertine composed of aragonite needle botryoids. The apron and channel facies (43–72°C) is floored by hollow tubes composed of aragonite needle botryoids that encrust sulfide-oxidizing *Aquificales* bacteria. The travertine of the pond facies (30–62°C) varies in composition from aragonite needle shrubs formed at higher temperatures to ridged networks of calcite and aragonite at lower temperatures. Calcite "ice sheets", calcified bubbles, and aggregates of aragonite needles ("fuzzy dumbbells") precipitate at the air–water interface and settle to pond floors. The proximal-slope facies (28–54°C), which forms the margins of terracette pools, is composed of arcuate aragonite needle shrubs that create small microterracettes on the steep slope face. Finally, the distal-slope facies (28–30°C) is composed of calcite spherules and calcite "feather" crystals.

Despite the presence of abundant microbial mat communities and their observed role in providing substrates for mineralization, the compositions of spring-water and travertine predominantly reflect abiotic physical and chemical processes. Vigorous CO_2 degassing causes a +2 unit increase in spring water pH, as well as Rayleigh-type covariations between the concentration of dissolved inorganic carbon and corresponding $\delta^{13}C$. Travertine $\delta^{13}C$ and $\delta^{18}O$ are nearly equivalent to aragonite and calcite equilibrium values calculated from spring water in the higher-temperature (—50–73°C) depositional facies. Conversely, travertine precipitating in the lower-temperature (<—50°C) depositional facies exhibits $\delta^{13}C$ and $\delta^{18}O$ values that are as much as 4‰ less than predicted equilibrium values. This isotopic shift may record microbial respiration as well as downstream transport of travertine crystals. Despite the production of H_2S and the abundance of sulfide-oxidizing microbes, preliminary $\delta_{34}S$ data do not uniquely define the microbial metabolic pathways present in the spring system. This suggests that the high extent of CO, degassing and large open-system solute reservoir in these thermal systems overwhelm biological controls on travertine crystal chemistry.

INTRODUCTION

The term "travertine", in its broadest sense, refers to all nonmarine carbonate precipitates formed in or near terrestrial springs, rivers, lakes, and caves (Sanders and Friedman 1967). Informal subdivisions include hot spring travertine (precipitates from high-temperature springs, also called carbonate sinters), tufa (precipitates from low-temperature springs, lakes, and waterfalls), and speleothems (precipitates from waters in low- to high-temperature subterranean caves or fracture systems (Pentecost 1995d; Ford and Pedley 1996). Minerals constituting these various types of travertine have crystal fabrics and compositions that are a sensitive environmental record of water chemistry, hydrologic transport, climate, and microbial populations. Travertine-related carbonates are therefore important data repositories for paleoenvironmental reconstructions. Examples include analyses of (1) speleothems lining the open fault zone of Devils Hole, Nevada, that have permitted the first high-resolution correlation of terrestrial and marine paleoclimatic histories (Winograd et al. 1988, 1992; Ludwig et al. 1992; Coplen et al. 1994); (2) speleothems associated with archeological studies that create benchmarks for age determinations and paleoclimatic reconstructions (e.g., Bar-Yosef and Kra 1994; Schwarcz et al. 1980; Schwarcz 1997; Bischoff et al. 1994); and (3) lacustrine tufa that gauges ancient lake level and paleoclimates in the Great Basin (Benson 1994; Benson et al. 1996)

The amplification, cloning, and sequencing of 16S rRNA genes in living microbes (Woese 1987; Stetter 1996; Pace 1997; Barns and Nierzwicki-Bauer 1997) suggests that the earliest common ancestor of life on earth was a high-temperature microbial organism. As a result, hot spring deposits have been identified as important targets in the search for ancient life on earth and other planets (Walter and Des Marais 1993; Farmer and Des Marais 1994a). Recent interest in hot spring travertine has been accelerated by suggestions that biogenic minerals and microfossils occur in Fe-rich carbonates of the Martian meteorite ALH84001, which are of possible hydrothermal origin (McKay et al. 1996). However, the potential use of travertine in reconstructing the early Earth biosphere and in the search for Martian life is hampered by the lack of a systematic process model for modern hot spring travertine deposition. The need for such a model is highlighted by the fundamental controversies surrounding the interpretation of water temperatures and potential microbial fabrics from carbonates in the ALH84001 meteorite (among others, McKay et al. 1996; McSween 1997; Valley et al. 1997).

This paper establishes a systematic facies model for the deposition of travertine by actively flowing hot springs at Angel Terrace, Mammoth Hot Springs, Yellowstone National Park. Travertine forms where subsurface waters erupt from the ground, cool, degas, and rapidly precipitate carbonate minerals with a variety of crystal morphologies and chemical compositions. Coupled water and travertine samples have been collected along spring discharge flow paths, petrographically described, and characterized with respect to their elemental and isotopic compositions. The resulting data have then been synthesized into a preliminary depositional facies model. The observed facies successions are used to track the aqueous–solid geochemical evolution of the spring system and directly link crystalline travertine fabrics with inorganic and organic controls on carbonate precipitation.

LOCATION AND GEOLOGICAL SETTING

Mammoth Hot Springs, near the northern boundary of Yellowstone National Park, Wyoming, U.S.A. (Fig. 1), is one of the world's largest sites

* Present Address: Department of Geology, Arizona State University, Box 870414, Tempe, Anzona 85287, U.S.A.

JOURNAL OF SEDIMENTARY RESEARCH, VOL. 70, No. 3, MAY, 2000, P. 565–585
 1073-130X/00/070-565/$03.00

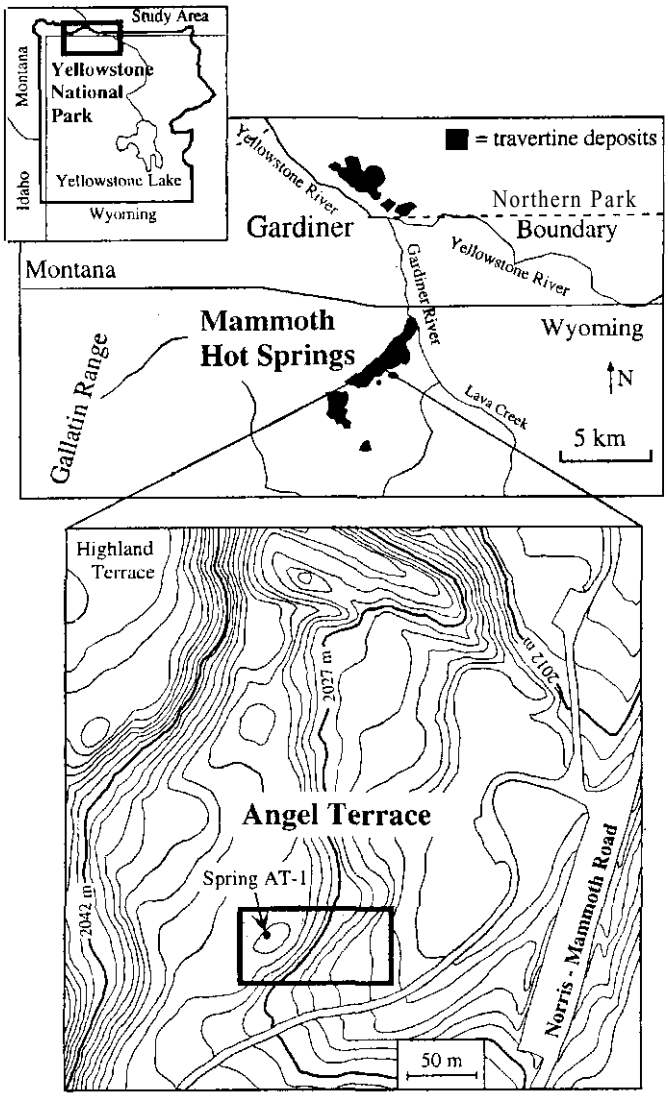

FIG. 1.-Geographic location of Mammoth Hot Springs in Yellowstone National Park. Wyoming. Map inset shows the location of Angel Terrace Spring AT-I within the New Highland area of Mammoth Hot Springs. Contour intervals are 1.5 m.

of active travenine accumulation. The travertine deposits of Mammoth Hot Springs are approxitnatcly 8.000 years old (Sturchio et al. 1992, 1994), 73 m in thickness, and cover more than 4 km^2 (Allen and Day 1935: White et al. 1975; Bargar 1978).Discharge from the entire Mammoth Hot Springs complex totals 590 l/s, uf which 10% erupts from the travertine terraces and 90% flows directly into the Gardiner River (Sorey 1991: Sorey and Colvard 1997). Regional groundwaters are heated by near-surface magma chambers and flow upward along the Mammoth and Swan Lake faults (Sorey 1991). The springs expel Ca–Na–HCO_3–SO_4 type hot waters with geochemically estimated subsurface reservoir temperatures of 100°C (Kharaka et al. 1991; Sorey and Colvard 1997).The thermal spring waters carry dissolved solutes derived from water–rock interaction with subsurface Paleozoic sedimentary rocks and are possibly mixed with waters derived from the Norris Geyser Basin (Sorey 1991; Sorey and Colvard 1997).

Travertine forms terraced and fissure ridge deposits. of which the terraces are the volumetrically dominant morphology at Mammoth Hot Springs (Bargar 1978). Angel Terrace, the site of the present study, is pan of the New Highland Terrace area. which comprises the southwestern part of the Mammoth Hot Springs complex (Figs. 1, 2; Peale 1883; Allen and Day 1935; Bargar 1978). Angel Terrace contains several small springs that are actively expelling water: the southwesternmost of thrsc is herein named Spring AT-I. The hydrologic system is dynamic, with multiple vents appearing, sealing, and reopening on Angel Terrace at a frequency of months to tens of years (Friedman 1970; Bargar 1978; Surcy and Colvard 1997).

PREVIOUS STUDIES

The geology and geomorphology of Mammoth Hot Springs has been described by Allen and Day (1935) and Bargar (1978). "Terraced travertine" accumulations are grouped into three size categories, which include terraces (tens of square meters), terracettes (a few square meters), and microterracettes (a few square centimeters or less). Friedman (1970) analyzed the isotopic compositions of spring water and travertine from Main Spring and New Highland Spring and concluded that cooling and CO_2 degassing were the dominant controls on the carbon and oxygen isotopic composition of the water and travertine. Chafetz and Lawrence (1994) also presented data for water and travertine from nearby Narrow Gauge Spring and observed that spring-water isotopic compositions were significantly different from those of the precipitated travertine. In 1967 the USGS drilled research hole Y-10 in New Highland Terrace (White et al. 1975; Sorey 1991). To date, however, no coupled petrographic and chemical analyses of travertine from the Y-10 core have been published. The most comprehensive analysis of Mammoth Hut Springs was a USGS study of the Corwin Springs geothermal area (Sorey 1991; Sorey and Colvard 1997). which includes anal-

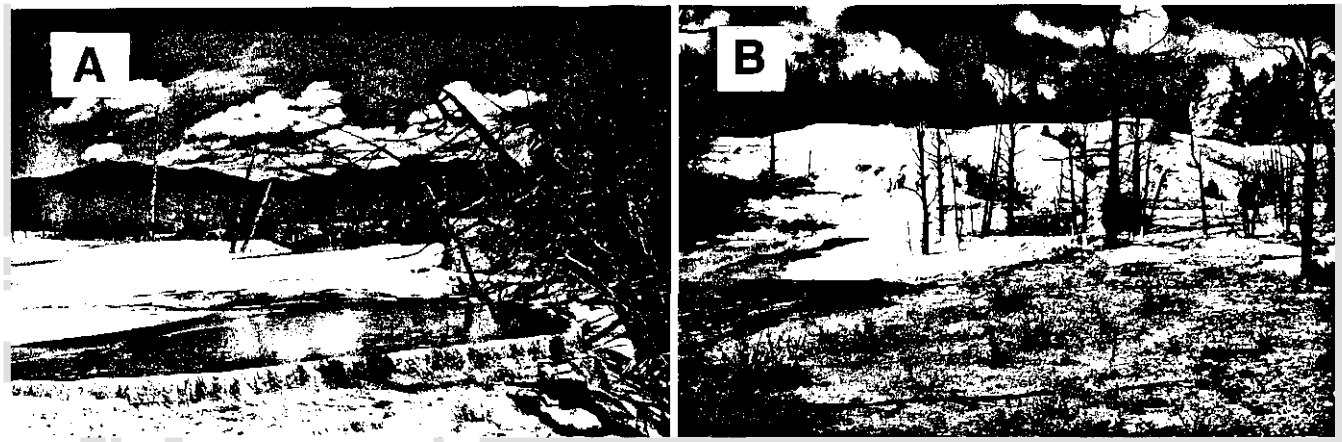

FIG. 2.—Field photographs of Angel Terrace Spring AT-I: A) view of the upper terracette pool, looking northward B) view of lhc proximal-slop and distal-slope facies, looking westward.

TABLE 1.—*Compilation of studies analyzing spring-water and associated travertine mineralization.*

Location	Morphology	Temp °C Low	Temp °C High	Water Chemistry	Travertine Chemistry	Travertine Mineralogy	Travertine Fabrics	Inferred Mechanisms	References (* denotes primary reference(s)
Angel Terrace and New Highland Terrace, Mammoth Hot Springs, Yellowstone, Wyoming	vents aprons channels pools terraces slopes	28.0	73.2	pH, TDC $\delta^{18}O$, $\delta^{13}C$ $^{87}Sr/^{86}Sr$ SO_4, $\delta^{34}S$	Ca, Mg, Mn, Sr, Fe, Mn, Na, Ti, S, Ba, V, P $^{87}Sr/^{86}Sr$ SO_4, $\delta^{34}S$	aragonite calcite	botryoids streamers shrubs raft sheets bubbles dumbbells blocky calcite	degassing evaporation	Fouke et al. (this paper)* Friedman (1970)*
Narrow Gauge, Mammoth Hot Springs, Yellowstone, Wyoming	fissure ridge	36.6	69.6	pH, alkalinity $\delta^{18}O$, $\delta^{13}C$	$\delta^{18}O$, $\delta^{13}C$	aragonite calcite	shrubs bubbles crusts	evaporation degassing	Chafetz and Lawrence (1994)*
Sardinia, Italy	channel waterfall	13.0	60.0	pH, alkalinity conductivity Ca, Mg, Na, K Ba, Sr, Mn, Fe Li, Cl, F, Si, Al SO_4, PO_4	Ca, Mg, Na, K Ba, Sr, Mn, Fe Li, Cl, F, Si, Al SO_4, PO_4	calcite dolomite quartz clay Fe-oxide	pisoids stromatolites	degassing microbial	Caboi et al. (1991)* Buccino et al. (1987)
Viterbo, Italy La Zitelle Springs Bagnaccio Springs	vent channel	34.0	61.0	pH, alkalinity $\delta^{18}O$, $\delta^{13}C$	$\delta^{18}O$, $\delta^{13}C$ Ca, Mg	aragonite calcite	shrubs spherulites crusts	evaporation degassing	Chafetz and Lawrence (1994)* Folk (1994) Gonfiantini et al. (1968)* Pentecost (1995a, 1995b)
Hot Tub Spring, Bridgeport, California Coast Range	channel	11.0	28.0	pH, alkalinity Ca, Mg, Na, K SO_4, Cl, F $\delta^{18}O$, $\delta^{13}C$	SiO_2 Fe Mn organic C $\delta^{18}O$, $\delta^{13}C$	siderite aragonite		degassing photosynthesis diagnesis	Amundson and Kelly (1987)* Barnes (1965) Barnes and O'Neil (1971) Chesterman and Kleinhampl (1991) Chafetz and Lawrence (1994)*
Valley md Ridge, Virgin-	waterfall	18.5	38.0	pH, alkalinity conductivity Ca, Mg, Na, K SO_4, Cl, F				mixing degassing	Herman and Lorah (1987, 1988)* Herman (1994)
Muschelkalk, Germany	channel waterfall	9.5	14.0	pH, alkalinity conductivity Ca, Mg, Na, K SO_4, Cl, F $\delta^{18}O$, $\delta^{13}C$	$\delta^{18}O$, $\delta^{13}C$	calcite		degassing precipitation	Usdowski et al. (1979)* Dandurand et al. (1982) Michaelis et al. (1985) Dreybrodt et al. (1929)
Durango, Colorado Rocky Mountains	mound channel	23.2	35.9	pH, alkalinity conductivity Ca, Mg, Mn Fe, Sr, K, Na SO_4, Cl $\delta^{18}O$, $\delta^{13}C$	$\delta^{18}O$, $\delta^{13}C$	aragonite calcite	bubbles rafts	microbial degassing	Chafetz et al. (1991a)* Chafetz and Lawrence (1994)*
Pagosa Springs, Colorado Rocky Mountains	mound	28.7	53.8	pH, alkalinity $\delta^{18}O$, $\delta^{13}C$	$\delta^{18}O$, $\delta^{13}C$	aragonite		bacterial	Chafetz and Lawrence (1994)*
Honey and Falls Creeks Oklahoma Arbuckle Mountains	waterfall	11.6	19.0	pH, alkalinity $\delta^{18}O$, $\delta^{13}C$	$\delta^{18}O$, $\delta^{13}C$	calcite	micritic crusts bushes, shrubs columnar	microbial degassing diagenesis	Chafetz et al. (1991b)* Love and Chafetz (1988, 1990) Chafetz and Lawrence (1994)*
Lake Bogoria, Kenya	vents pools	69.0	99.0	pH, alkalinity Ca, Mg K, Na, Li, F, I SO_4, Sl, SiO_2 $\delta^{18}O$, $\delta^{13}C$	$\delta^{18}O$, $\delta^{13}C$	calcite aragonite oxides dolomite	botryoids dendrites	temperature degassing diagenesis microbial	Renaut and Jones (1996)* Jones and Renaut (1996a, 1996b)

yses of travenine and spring water from New Highland Terrace (Kharaka et al. 1991; Sturchio 1990; Sturchio et al. 1992). Uranium-series age determinations from this work indicate that deposition of the travertine deposits in nearby Gardiner, Montana (Fig. 1), was interrupted and that the deposits were partially eroded by glacial advances during the late Pleistocene (Pierce et al. 1991; Sturchio et al. 1994).

Angel Terrace hot springs have also been used to study the influence of microbial communities on the precipitation of laminated (stromatolitic) travertine fabrics (Farmer and Der Marais 1994b). This work identified the following general relationships along the spring outflow channels. Above 74°C, cyanohacteria are excluded because of thermal intolerance. and only biofilms of hyperthermophilic archaehacteria and bacteria persist. Between approximately 70 to 74°C, carbonate precipitation occurs as radial growths of microfibrous aragonite encrusting filamentous sulfide-oxidizing bacteria. This bacterium was previously identified as *Thermothrix* (Brock 1978) but is now interpreted as belonging to the *Aquificales* group (A.L. Reysenbach, personal communication). At temperatures below ~55°C, microbial mats form that consist of a diverse association of photosynthetic cyanohacteria (Farmer and Des Marais 1994b).

Several studies have analyzed hoth aqueous and solid-phase components of terrestrial groundwater springs (Table 1j. Results indicate that the primary controls on travertine precipitation are a complex interplay of water chemistry (e.g., pH, HCO_3. pCO_2, elemental abundance, and resultant saturation state). physical processes (e.g., temperature change, degassing, boiling. steaming. evaporation, and dilution), hydrology (e.g., flow rates and surface area). and biotic activities (e.g., photosynthesis and respiration). Small diurnal differences in isotopic ($\delta^{13}C$ and $\delta^{18}O$) composition have been observed in spring waters (Amundson and Kelly 1987; Chafetz et al. 1991a; Chafctz et al. b: Pentecost 1995b). Travertine precipitated from modern hot springs is composed of aragonite and solid solutions of low-Mg to high-Mg calcite (Barnes and O'Neil 1971). These metastable mineralogical compositions make travertine susceptible to extensive diagenesis, and it is presumed that these alterations begin soon after deposition (Cipriani et al. 1977; Chafetz and Folk 1984; Folk et al. 1985; Love and Chafetz

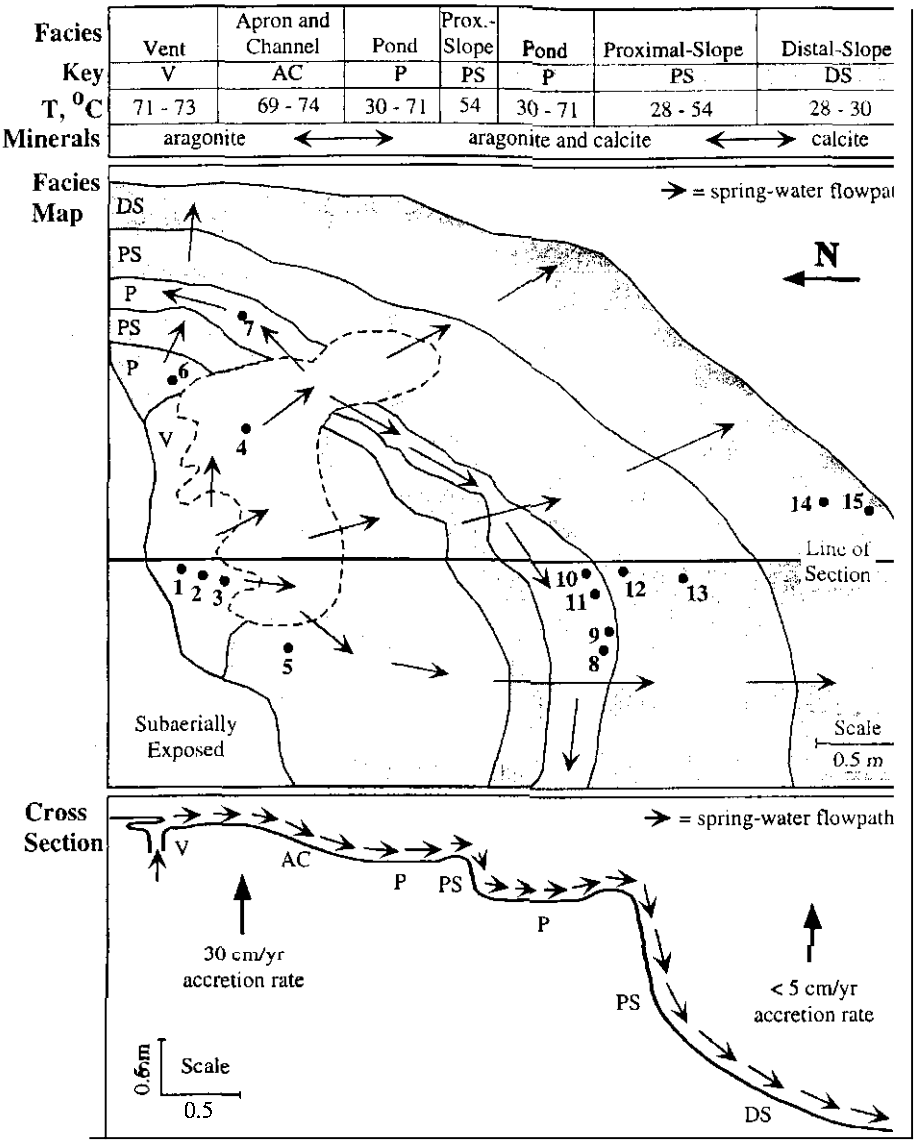

FIG. 3.—Facies map and cross section of Angel Terrace Spring AT-1, indicating spring-water temperatures, travertine mineralogy, facies distributions, flow directions, and the positions of samples 1 through 15. Facies abbreviations include: (1) vent facies (V), (2) apron and channel (AC) facies, (3) pond facies (P), (4) proximal-slope facies (PS), and (5) distal-slope facies (DS).

1988, 1990; Guo et al. 1996). Isotopic equilibrium between travertine and the spring water from which it precipitates is often not attained in subaerial hot springs because of kinetic effects associated with CO_2 degassing and high rates of precipitation (Usdowski et al. 1979). CO_2 degassing causes supersaturation with respect to carbonates, an effect that is further enhanced by generally high Ca concentrations (Usdowski et al. 1979). Degassing and precipitation take place simultaneously, with the rate of precipitation accelerating with the cumulative extent of degassing (Dreybrodt et al. 1992).

Despite the work highlighted above, the classification and interpretation of hot spring travertine remains controversial and fundamentally unresolved. One reason for this is the extreme spatial and temporal variability in the mineralogy and geochemistry of these deposits (Usdowski et al. 1979; Amundson and Kelly 1987; Jones et al. 1998; Chafetz et al. 1998). Existing schemes group travertine according to the origin of their CO_2 (Pentecost and Viles 1994; Pentecost 1995d) and the water temperature at which they are precipitated (Pedley 1990; Ford and Pedley 1996). However, these classification schemes do not directly correlate water chemistry with changes in the crystallization fabric and composition of travertine along the spring drainage systems.

METHODS

Field sampling of the Angel Terrace spring waters and travertine was completed from a single sample set collected during daylight on 13 May, 1997. The 1-cm-thick uppermost surface of the travertine and the associated spring waters were systematically sampled along flow paths running from the spring vent to the distal parts of Angel Terrace Spring AT-1 (sample positions are shown in Figure 3). Travertine was collected with a knife and spatula and later impregnated with Araldite 506/Sympoxy CA-803 low-viscosity epoxy under high vacuum for sectioning. Water samples were filtered using 0.22 μm mesh annealed Whatman GFF filters, collected in triplicate in three-times acid-washed glass bottles, acidified with HCl, filled to capacity leaving no head space to prevent degassing, and poisoned with 0.1 ml of a saturated solution of $HgCl_2$ to prevent biological activity. The samples were then transported and stored in a darkened refrigerated cooler until analysis.

The water samples were analyzed for dissolved inorganic carbon (DIC, dissolved $CO_3 + CO_2^- + H_2CO_3 + HCO_3^-$) and carbon isotopes. Aliquots of sample water (3 ml) were transferred by syringe to an evacuated

TABLE 2.—*Crystal fabrics and large-scale morphologies comprising the Angel Terrace Spring AT-1 travertine depositional facies.*

Facies	Morphology	Basic Components	Micron-Scale Fabrics	Centimeter- to Millimeter-Scale Fabrics
Vent	spring orifice	aragonite needles (≤100 μm)	botyroidal clusters	hemispherical mounds (<1 cm–10 cm)
Apron and Channel	primary outflow conduits	aragonite needles (≤100 μm)	botyroidal clusters	streamers (1–5 mm × ≤ 30 cm)
Pond	terrace pools	aragonite needles (≤100 μm)	dendritic clusters	shrubs (≤1 cm)
		block calcite (50–100 μm)	fuzzy dumb bells	ridged networks (≤2 cm)
				ice sheets (1–2 mm thick)
				calcified bubbles (0.5–3 mm)
Proximal-Slope	terrace margins	aragonite needles (≤100 μm)	dendritic clusters	arcuate shrubs (≤2 cm)
	microterracettes	blocky calcite (50–100 μm)	fuzzy dumb bells	ice sheets (1–2 mm thick)
				calcified bubbles (0.5–2 mm)
Distal-Slope	laminated crusts	blocky calcite (25–100 μm)	dendritic clusters	shrubs (≤1 cm)
	microterracettes			spherulites (≤3 mm)
				calcified bubbles (0.5–2 mm)

130 ml Wheaton bottle and acidified with 0.2 ml of "102%" phosphoric acid. The phosphoric acid was prepared by evaporating reagent-grade 85% phosphoric acid under vacuum until it contained a small concentration of anhydrous phosphoric acid. This procedure eliminates potential contaminants, such as N_2O. After the acidified sample equilibrated for 20 min, gases in the head space of the bottle were drawn into a vacuum line. To remove water, the gas was drawn through a methanol–dry ice cold trap (−70°C) and a variable-temperaturc cold trap (Des Marais 1978) held at −127°C. The CO_2 was then trapped at −196°C. The CO_2 was measured using a mercurj manometer and then flame sealed in a Pyrex (Coming Glass Works) tube, 6 mm in diameter and 10 cm long, for isotopic analysis. Carbon-isotope measurements were performed using a Nuclide 6–60RMS mass spectrometer modified for small-sample analysis (Hayes et al. 1977). All isotopic results are reported as per mil values relative to the Peedee belemnite carbonate standard using the standard delta notation $\delta^{13}C = [(R_{sample}/R_{standard}) - 1] \times 1000$, where $R = {}^{13}C/{}^{12}C$ and $R_{standard} = 0.0112372$. For the overall procedure, the 95% confidence limits for $\delta^{13}C$ were 0.2.

Polished thin sections were examined with plane-polarized light and under cathodoluminescence on a CITL Cold Cathode Luminoscope operating at 11 kV and 500 μA. Travertine chips were either carbon- or iridium-coated and analyzed on a JEOL JSM 25S SEM operating at 15 kV. Coordinated plane-light. cathodoluminescence, and SEM photomicrograph mosaics were constructed to serve as guides for microsample drilling to avoid diagenetically altered portions of the travertine (Popp et al. 1986; Fouke et al., 1996). The mineralogical composition of each specimen was determined using X-ray powder diffraction (XRD). Samples were ground under acetone. and smear mounts were prepared. The XRD data were collected on a Rigaku MiniFlex automated powder diffractometer using Cu $K\alpha$ radiation (30 kV, 15 mA), which was calibrated using an external Si standard. Data were collected over the range of 3 to 65° 2θ.

Travertine carbon- and oxygen-isotope analyses were measured on the CO, released during digestion of 20 to 50 μg of powdered travertine in 100% phosphoric acid at 50°C on a Finnigan-Mat mass spectrometer. Data are reported as $\delta^{13}C$ values for CO, gas relative to PDB using the standard delta notation, and $\delta^{18}O$ is reported relative to SMOW (Craig 1957). Analytical precision was 0.1 per mil for oxygen and 0.2 per mil for carbon. *In situ* elemental abundances were obtained by electron probe microanalysis (EPMA) on a Camex 50×, operating at 20 kV and 0.015 μA with a beam 10 μm in diameter. Estimated precision is expressed as 95% confidence limits and is typically better than 2% for major elements and 4% for trace elements as calculated from replicate analyses.

Solid-phase sulfate concentrations and corresponding sulfur-isotope values were determined using 10 g of poadered travertine that were placed in a N_2-purged flask followed by a slowly stirred addition of 80 ml of 6N deoxygendtrd HCI while bubbling the solution with N_2. After boiling and cooling, dissolved SO_4 was retained in the acidic solution and evolved H_2S was flushed from the flask in a stream of N_2. The residual insoluble sediment and the acidic solution were filtered. and the acidic solution was diluted to 500 ml with double-distilled deionized water (DDI) and then evaporatively concentrated to 200 ml while keeping the solution below the boiling pint. Approximately 20 ml of saturated $BaCl_2$ solution was added. and the solution was evaporatively concentrated to 75 ml. $BaSO_4$ precipitated overnight at room temperature was filtered and dried at 65°C. Slow evaporation of this large volume of solution enhances $BaSO_4$ crystal growth and the efficiency of retention of the precipitate on the filters. It is uncertain whether the travertine sulfate was substituted into the crystal lattice or trapped within fluid or solid inclusions. Sulfate yields were determined

TABLE 3.—*Geochemical composition of Angel Terrace Spring AT-1 water.*

Travertine Sample No	Water Sample No	Lithofacies	Depth cm	Temp °C	Range °C	pH	TDC mg/l	6°C ‰ PDB	$\delta^{18}O$ ‰ SMOW	$^{87}Sr/^{86}Sr$	SO_4 mg/kg	$\delta^{34}S$ CDT	Water Depth cm	Relative Flow rate
970513-1	970519 1A	vent	3.2	73.2	71–74	6.0	192	−0.9	−18.1	071127	518	19.6		
970513-2		vent	3.2	73.2		6.0							≤1–5	high
970513-3		vent	2.6	71.0										
970513-4	970519.2A	apron and channel	2.8	43.7	69–74	7.5	111	1.0	−17.7		522	19.9	≤3	high
970513-5	970519.3A	pond	3.0	62.2	30–71	5.8	135	0.4	−17.9		522	21.0		
970513-6		pond	2.1	43.7		7.5								
970513-7		pond	3.6	46.9		6 9								
970513-8		pond	3.4	10.1		7 9							≤5	low
970513-9		pond	3.4	30.1		7.9								
970513-10		pond	1.4	60.0		1.4								
970513-11		pond	0.5											
970513-12	970519.4A	proximal-slope	0.5	54.2	16–65	7.4	111	1.6	−18.3		547	20.0		
970513-13a	970519.5A	proximal-slope	0.5	28.0			97	3.0	−17.1		519	19.1	61	moderate
970513-13b		proximal-slope	0.5											
970513-14	9709519-6A	distal-slope	0.5	30.2	16–45	8.0	75	4.6	−11.1	0.71110	537	206.6	≤1	low
970513-15	970513 7A	distal-slope	0.5	30.2		8.0								

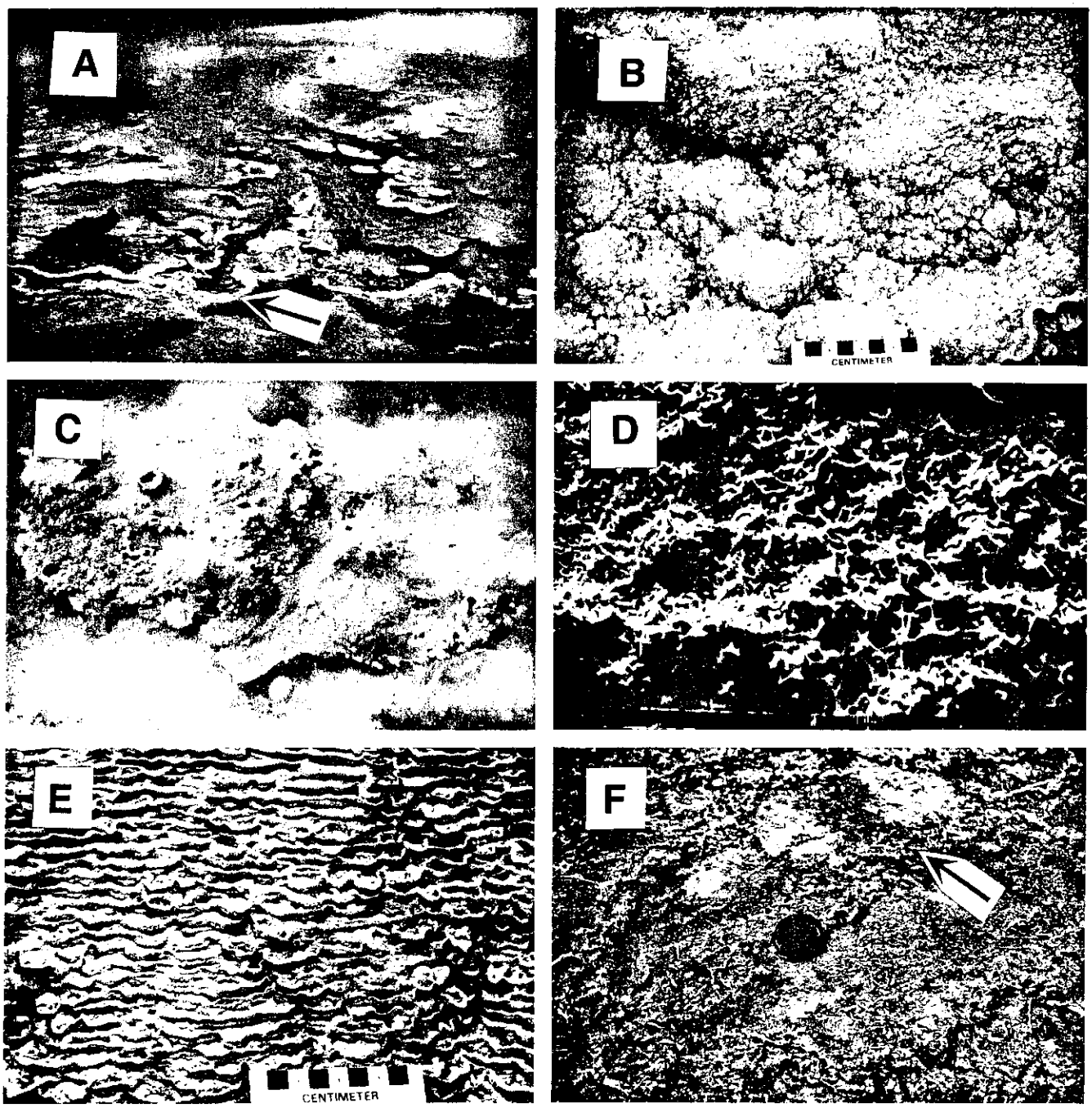

FIG. 4.—Field photographs of Angel Terrace Spring AT-1: A) vent, apron and channel, and pond facies (arrow shows position of orifice); B) aragonite needle shrubs flooring the pond facies; C) Calcite "ice sheets" and calcified bubble on the surface of spring-water in the pond facies (field of view is 10 cm); D) ridged networks in the pond facies (field of view is 10 cm); E) well-developed microterracettes on the steep outer face of the proximal-slope facies; and F) broad microterracettes containing calcified bubbles and plant material in the distal-slope facies.

gravimetrically and then checked by gas volume during combustion and cryogenic purification. Reproducibility of gravimetric determinations was generally ±2% of the reported value. Elemental sulfur was extracted from rock powder by refluxing dichloromethane in a Soxlet apparatus followed by precipitation of the solubilized elemental sulfur on activated granular copper. Yield of elemental sulfur is considered to be trace level if the surface of the granular copper is altered to a metallic bluish black but not completely coated by an opaque black sulfide layer.

Spring water (7.5 ml) was diluted to 500 ml with DDI water, which was concentrated by evaporation at a gentle boil to 200 ml, followed by addition of 20 ml of $BaCl_2$. Precipitation and recovery of $BaSO_4$ was repeated as before. A 1:1 mixture of V_2O_5/SiO_2 was used as the oxidant and added in a 20:1 weight ratio to minimize isotopic shifts during $BaSO_4$ combustion for isotopic analyses. Native copper turnings (triple cleaned with 1N HCl and dicholoromethane) were added to the sample to remove excess oxygen during combustion and prevent formation of SO_3 gas.

Isotopic analyzes were performed on SO_2 gas that was obtained by combusting the $BaSO_4$ at 102.5°C for 20–30 minutes on a vacuum line, with

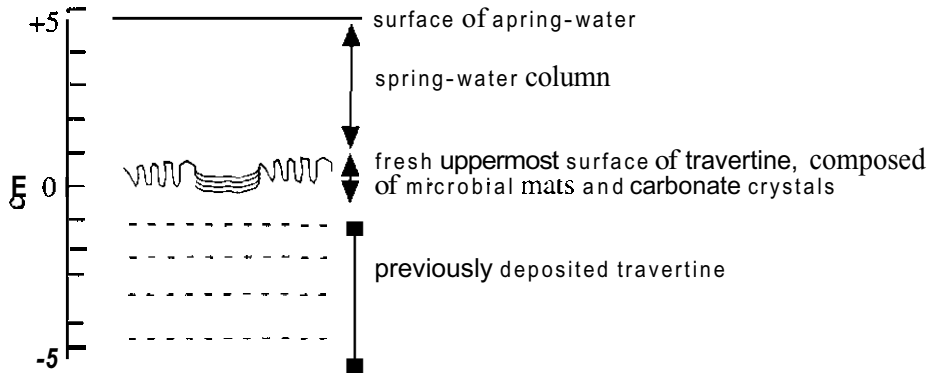

FIG. 5.—Sketch of the uppermost surface of travertine accumulation in the pond facies, illustrating the spatial relationships between actively flowing spring water, fresh travertine with microbial mats, and underlying older travertine.

collection of the evolved purified gases in a cryogenic trap. Evolved CO, was removed at −187°C to −145°C. Evolved SO, was transferred at −145°C to −95°C to a second cryogenic trap, quantified manometrically, sealed in 6 mm o.d. borosilicate tubes, and analyzed on a Nuclide 6–60 mass spectrometer. Precision of isotope analyzes for replicated samples and laboratory standards was 0.25‰. Data are expressed in standard $\delta^{34}S$ per mil notation relative to Canyon Diahlo Troilite (CDT).

Strontium-isotope ratios of spring water and travertine were measured on a Finnigan-MAT 261 fixed multicollector thermal ionization mass spectrometer. Ten replicate analyses of NBS SRM 987 yielded a $^{87}Sr/^{86}Sr$ mean value of 0.71025 with a standard deviation for any one analysis of 0.000015. Average in-run precision was ±0.000015 for the standard and ±0.000015 for each sample.

COMPOSITION OF THE ANGEL TERRACE SPRING SYSTEM

Angel Terrace Spring AT-1 is composed of a series of shallow-water environments distributed along drainage How paths running from the spring orifice to the distal pans of the system. These aqueous environments and their associated travertine deposits are divisible into five laterally distributed depositional facies on the basis of water temperature and chemistry. travertine crystalline fabric. and travertine chemistry (1) vent facies, (2) apron and channel facics. (3) pond facies, (4) proximal-slope facies, and (5) distal-slope facies (Table 2; Figs. 3, 4). Travertine precipitated in each of the depositional facies exhibits distinct crystallographic characteristics. which in turn control the large-scale morphology and stratigraphy of the overall travenine deposit.

Three vertically stacked subenvironments are present at any one location in each facies: (1) the overlying shallow [1 to 15 cm water depth] layer of spring water. (2) the fresh. actively precipitating uppermost travertine surface [≤ 1 cm depth] with living micrnbial mats, and (3) travenine at depths greater than 1 cm below the upper accretionary surface (Fig. 5). Analyses in this study have been limited to the spring water and the uppermost 1 cm-thick accretionary surface of the travertine to minimize historical variations. Spring vents are self-sealing and migrate laterally over time periods of several months to years (U.S. Park Service Rangers, personal communication), leading to frequent lateral shifting of the depositional environments. Therefore, it is possible that the travenine occurring just below the uppennost surface of accumulation may not have been precipitated from the actively flowing spring water. However. preliminary crystallization substrate experiments (stainless steel washers placed in each depositional environment for approximately 48 hours) suggest average precipitation rates of at least 30 cm/year in the vent, apron and channel, and pond facies and less than 5 cm/year in the distal-slope facies. As a result, the uppermost 1-cm-thick surface of the travertine could accumulate in as little as 15 to 15 days. These durations are significantly shorter than the time scales of several months to years at which vents and outflow paths shift. This suggests that the uppermost 1 cm of uniformly crystalline travertine was prccipitatcd from the spring waters currently flowing over each site of travertine deposition.

System Overview

Spring water emerges from the ground in the vent facies through an irregularly shaped 5-ctn-diameter orifice (Figs. 3, 4A; Bargar 1978). The water exhibits a rolling flow as it is expelled because of vigorous CO, outgassing. The strong sulfidic odor for which these springs are well known indicates that H_2S gas is also being released. The vent water steams as it leaves the conduit through mushronm-shaped travertine accumulations that accrete to the air–water interface (Fig. 4A). Spring waters then flow rapidly through the gently sloped apron and channel facies (Fig. 3), followed by deceleration and accumulation in the pan-shaped pond facies. The pond margins are characterized hv raised rims of travertine up to 10 cm high, forming terracettes several meters in diameter (Figs. 2A, 3; Bargar 1978).

Angel Terrace Spring AT-1 is composed of upper and lower juxtaposed terracettes (Fig. 3). Warm spring water from the apron and channel facies enters the upper pond laterally and mixes with pond water that has begun to cool (Fig. 3). The lower pond also receives cooler water cascading over the upper proximal-slope facies (Fig. 3). This mixing of water creates a 36°C range in water temperature in the pond facies (Fig. 3). However, the time periods over which this is sustained is uncertain. Spring water then cascades over the steep proximal-slope facies as a pulsating sheet Row. Small microterracettes, 1 to 3 cm in diameter, cover the slope of the proximal-slope facies (Fig. 4E). Spring water then continues to flow down into the low-inclination distal-slope facics, where the water velocity slows and broad microterracettes up to 10 cm in diameter are formed (Fig. ##.

Aqueous Geochemistry

The depth, temperature, pH, and isotopic composition of the water in each facies are presented in Table 3. Water temperature decreases from 73°C to 28°C along the spring outflow (Fig. 3). The observed departures from a smooth thermal gradient with increasing distance from the vent are caused by the particular How patterns and water depth of each facies (Fig. 3). Spring water pH increases along the How paths from 6.0 at the vent to 8.0 in the dish-slope (Fig. 6A). This is acconipanied by a large (+117 mg/l) decrease in total dissolved inorganic carbon (DIC; Fig. 6C) and a simultaneously large increase in $\delta^{13}C$ from −1 to +5‰ PDB (Figs. 6B, C. 7). Conversely. the water $\delta^{18}O$ exhibits only a small increase from −18.3 to −17.1‰ SMOW across the same flow path (Fig. 6D, E). Variations in dissolved strontium $^{87}Sr/^{86}Sr$ are extremely small, exhihiling a downflow increase of only 0.00017 (Fig. 6F). Variations in dissolved sulfate (518 to 547 ppm) and its associated $\delta^{34}S$ signature (19.6 to 20.6‰ CDTJ in the spring waters are both relatively invariant from the vent to distal-slope facies (Fig. 6G, HJ.

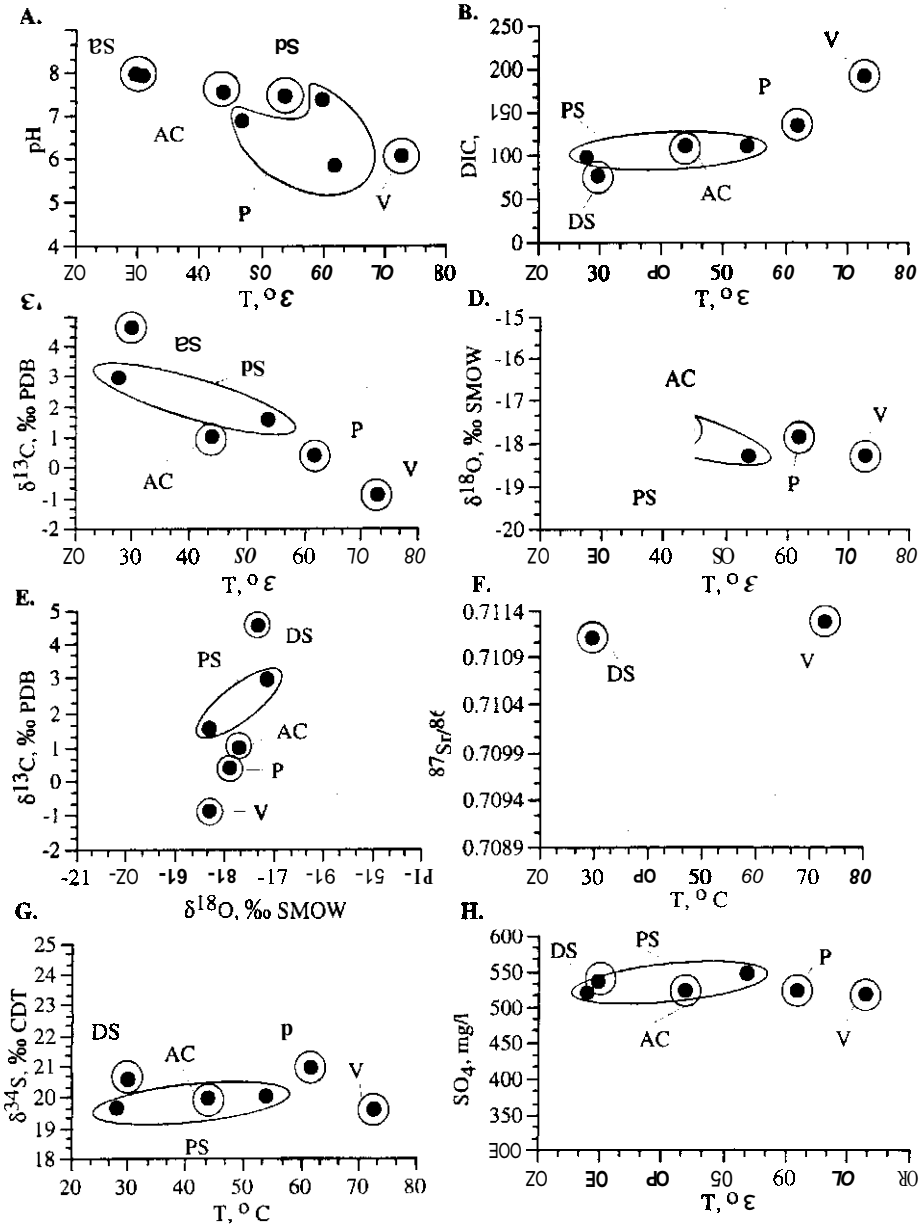

FIG. 6.—Covariation plots of Angel Terrace Spring AT-1 water chemistry. Isotope analyses in Part E represent sum CO_2. Data are presented in Table 3. The vent (V), apron and channel (AC), pond (P), proximal-slope (PS) and distal-slope (DS) depositional facies from which the data were collected are indicated.

Travertine Fabrics, Mineralogy, and Stratigraphy

The Angel Terrace travertine is composed of three basic crystalline building blocks: (1) aragonite needles up to 200 μm in length, (2) microcrystalline calcite less than 5 μm in diameter, and (3) blocky to prismatic calcite crystals 30 to 100 μm in diameter. These crystals are organized into a variety of larger-scale crystal growth patterns that change systematically along the spring water flow path. Travertine precipitated in the vent facies is composed of botryoids of acicular aragonite needles (10 to 100 μm in diameter). The botryoids nucleate on dark elongate microcrystalline calcite cores that are interpreted as bacterial filaments (Fig. 8A; Farmer and Des Marais 1994b). The botryoids encrust each other to form mushroom-shaped hemispherical mounds (0.5 to 10 cm in diameter) that typically build to the water–air interface and are periodically exposed to the atmosphere (Fig. 4A). Rare patches of blocky calcite crystals (100 μm in diameter), observed in the botryoids (Fig. 8B) represent either primary precipitates or diagenetic alteration of primary aragonite. The apron and channel facies is floored by sinuous microbial mats composed of sulfide-oxidizing filamentous bacteria (*Aquificales* group). Aragonite precipitates on the surface of these bacterial filaments to form carbonate tubes that reach a few millimeters in diameter and tens of centimeters in length. The microbial filaments rapidly degrade, leaving hollow tubes with an inner thin layer of microcrystalline calcite that is encrusted by large aragonite needle botryoids (Fig. 8C).

Several different aragonite and calcite travertine fabrics occur in the pond facies. At the highest temperatures (58–70°C), aragonite needles grow upward from the pond floors in a variety of shrub-like forms that reach 1 cm in height (Figs. 4B, 8E; Bargar 1978; Pentecost 1990). Lower-temperature pond floors (43–57°C) are covered with mats of the microbe *Spirulina* (Brock 1978), forming ridged networks of microcrystalline calcite 1 to 2 cm high encrusted with large blocky calcite crystals (Figs. 4D, 8D). On the surfaces of both the high and low temperature ponds, calcified bubbles and 100-μm-thick carbonate "ice sheets" precipitate at the air–water interface (Figs. 4C, 9A–D; Allen and Day 1935; Bargar 1978; Chafetz et al. 1991a). The bubble walls and ice sheets are composed of microcrystalline

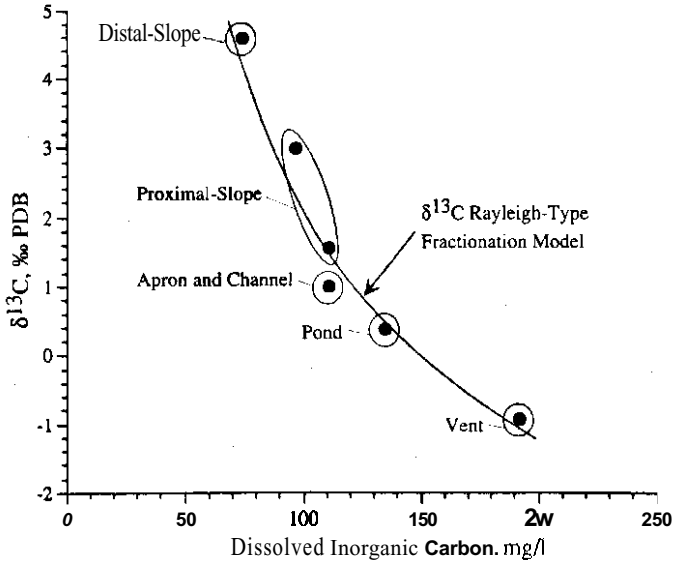

FIG. 7.—Covariation plot of spring-water total dissolved inorganic carbon (DIC) versus its $\delta^{13}C$ value. Angel Terrace Spring AT-I data are consistent with modeled Rayleigh-type fractionation, calculated using equations presented in Usdowski et al. (1979), Michaelis et at. (1985), and Amundson and Kelly (1987). Calculations are described in the text.

calcite. The bubble inner walls and ice-sheet upper surfaces are smooth (Fig. 9A–D). In contrast, the outer bubble walls and lower ice sheet surfaces act as nucleation sites from which 50 to 100 μm blocky calcite crystals and small (<15 μm) acicular aragonite grow. The aragonite forms botryoids as well as dumbbell-shaped aggregates composed of parallel needles that spread at their ends into radiating hundles ("fuzzy dumbbell" of Folk et al. 1985; Folk 1993, 1994; Buczynski and Chafetz 1991; Chafetz and Buczynski 1992). Some of these fuzzy dumbbells are flat on one side, suggesting that they grew at the air–water interface. Conversely, others are three-dimensional rather than flat on one side and may represent precipitation in the water column or on the pond floor. The calcified bubbles and ice sheets are blown by the wind across the pond water surface, sink, and accumulate on the pond floor as well as against the inner edge of the pond rim. Thicker ice sheets form when a pond slowly desiccates after migration of the spring vent cuts off water inflow (Allen and Day 1935; Bargar 1978).

The proximal-slope facies begins at the top of the pond rim and forms the high-angle (45" to 85" inclination) outer face of the terracette, creating buttresses up to 1.5 m in height (Fig. 2A). The proximal-slope travertine is composed of aragonite needles organized into shrub-like growth structures that are either linear or concave upward (Fig. 8F). These arcuate, dendritically branching crystal aggregates form the microterracettes on the outer face of the proximal-slope travertine (Fig. 8E; Chafetz and Folk 1984; Guo and Riding 1992). Travertine precipitating in the distal-slope facies is composed of two distinct types of crystal growth. The first are detidritic "feather crystals" growing on the floors of microterracette ponds (Fig. 4F) composed of branching stalks of ≤10 μm blocky to prismatic crystals of calcite (Fig. YE; Chafctz and Folk 1984; Folk et al. 1985; Guo and Riding 1992). The second consists of irregular spherules up to 0.5 cm in diameter composed of ≤50 μm euhedral calcite crystals and clumps of microcrystalline calcite (Fig. 9F). Detrital pieces of ice sheets, calcified bubbles, and furry dumbbells also occur in the proxinial and distal-slope facies, which have been suspended in the shallow water column and washed downstream from the pond facies.

The stratigraphic patterns created during travertine accumulation are extremely complex because of constant lateral changes in vent position and hydrologic inflow and outflow along the spring system. However, the two-step terracette morphology of the Angel Terrace Spring AT-I travertine likely represents a comhination of at least two end-member accretionary models. The first is a downstepping mechanism in which the upper terracette is older. and the lower terracette onlaps the previous deposits of the proximal-slope and distal-slope facies (Fig. 10A). If caused by an increase in spring outflow without change in the location of the vent, this would be accompanied by lateral progradation of the apron and channel facies over the previous pond and proximal-slope facies. The second is a backstepping mechanism in which the lower terracette is older, and the upper terracette has built out over the top of the original terracette (Fig. 10B). Cross-sectional exposures or cores through the Angel Terrace Spring AT-I deposits will be necessary for evaluation of these models.

Travertine Geochemistry

The elemental and isotopic compositions of the Angel Terrace travertine are presented in Tables 4 and 5. Travertine in the vent facies and apron and channel facies is composed of aragonite. Waters in the pond and proximal-slope environments precipitate travertine composed of a mixture of aragonite and calcite. Travertine precipitated in the distal-slope is composed almost entirely of calcite (Fig. 3). Both the $\delta^{13}C$ (2.7 to 5.2 ‰ PDB) and $\delta^{18}O$ (4.0 to 8.6 ‰ SMOW) values exhibit a significant increase along the spring How path (Fig. 11A, B). Sulfate abundance (2.940 to 20,840 ppm) increases by nearly an order of magnitude across the spring drainage system (Fig. 1 IC), yet the travertine sulfate $\delta^{34}S$ (21.5 to 24.1 ‰ CDT) is virtually invariant (Fig. 11D). Sr abundance (619 tu 2556 ppm) is greatest in the high-temperature aragonitic travertine (Fig. 11E), whereas $^{87}Sr/^{86}Sr$ (0.71110 to 0.71112) shows nu variation from vent to distal-slope (Fig. 11F). Mg abundance (30 to 4891 ppm, or 0 to 2 mol %) is consistently low in the higher-temperature facies and is variable in the lower-temperature facies (Fig. 11G). Sodium concentrations (58 to 580 ppm) exhibit a gradual increase across the spring system (Fig. 11H). Travertine Fe and Mn abundances exhibit small (+100 to 150 ppm) but significant downflow increases (Fig. 12A, B) and are more variable in the distal facies. Elemental sulfur increases from 630 to 5288 ppm from vent to distal-slope (Fig. 12C), and Ba (35 to 245 ppm) exhibits variable hut low concentrations (Fig. 12D).

DISCUSSION

Significant modification of the spring water takes place during expulsion at the vent and progressive drainage through the apron and channel, pond, proximal-slope, and distal-slope facies. The chemical, physical, and biological processes along the spring outflow and their influence on travertine chemistry and fabric are evaluated in the following sections.

Subsurface History of the Spring Waters

Chemical and isotopic analyses from throughout the Mammoth Hot Springs complex suggest that the subsurface water at Angel Terrace is derived from a combination of: (1) meteoric waters sourced from the Gallatin Range and/or the Beartooth Uplift to the north and transported into the subsurface along major fault systems and (2) deep lateral flow of Norris Basin waters from the south (White et al. 1975: Kharaka et al. 1991; Sorey and Colvard 1997). Values of $^{87}Sr/^{86}Sr$ and $\delta^{34}S$ in Angel Terrace spring water and travertine (Figs. 6, 11) are consistent with those reported by Kharaka et al. (1991) for other springs in the Mammoth Hot Spring curridor. These compositions are indicative of subsurface water–rock interactions with limestones and anhydrites of the Mississippian Madison Group (Kharaka et al. 1991). The small amount of deuterium fractionation relative to meteoric water measured at spring orifices (+0.2 to +0.4‰ $\Delta\delta D$ SMOW; Friedman 1970; Kharaka et al. 1991) suggests that the subsurface spring waters have experienced relatively little boiling prior to expulsion at the surface.

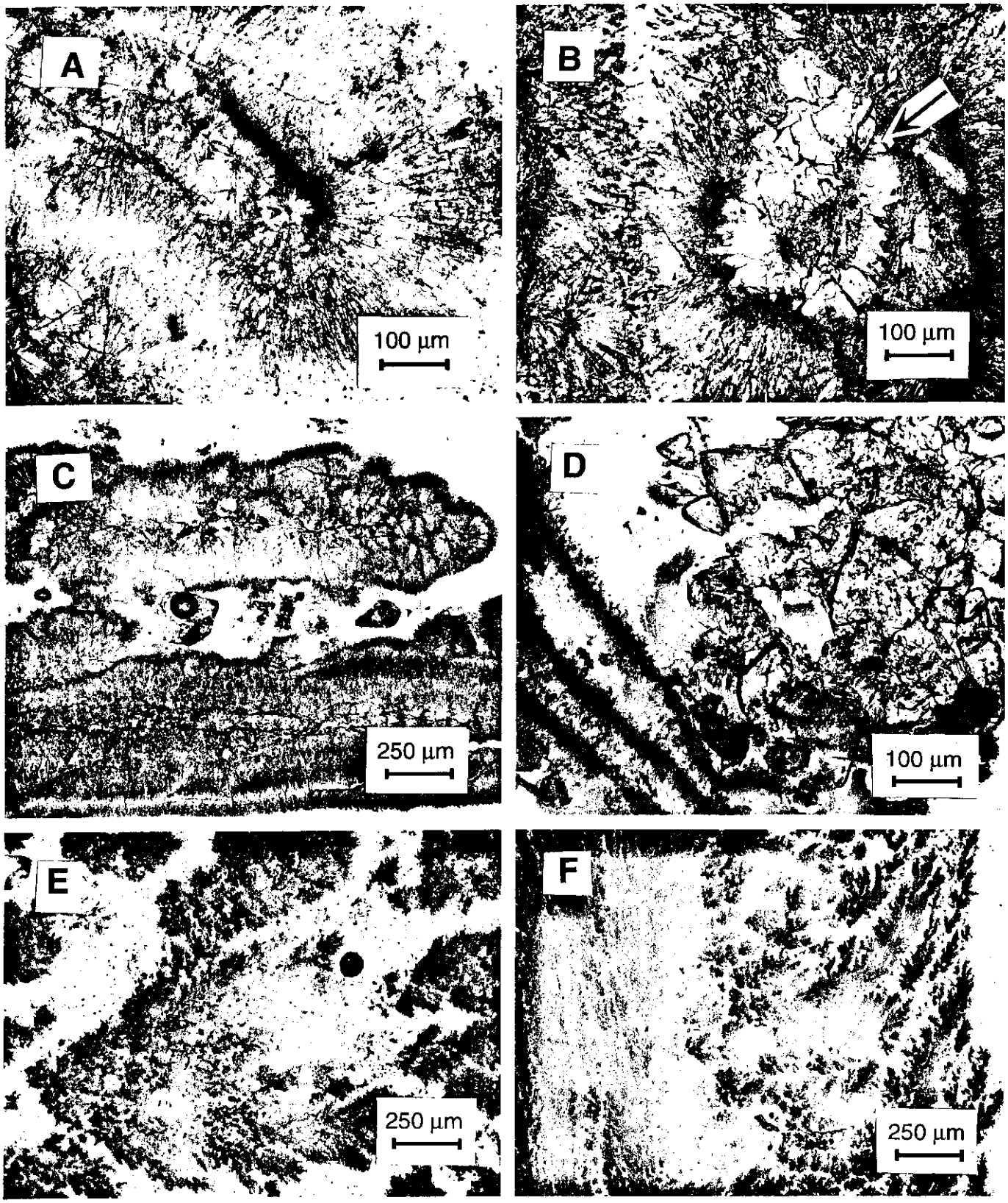

FIG. 8.—Photomicrographs of travertine facies at Angel Terrace Spring AT-1: **A)** aragonite needle botryoids in the vent facies; **B)** rare patch of calcite replacement or inversion in aragonite needle botryoids of the vent facies; **C)** streamer walls composed of aggregates of aragonite needle botryoids in the apron and channel facies; **D)** blocky calcite crystals, thin microcrystalline calcite walls, and small encrusting aragonite needles in ridged networks constituting the pond facies; **E)** dendritic aragonite needle shrubs in the pond facies; **F)** arcuate aragonite needle shrubs constituting the proximal-slope facies.

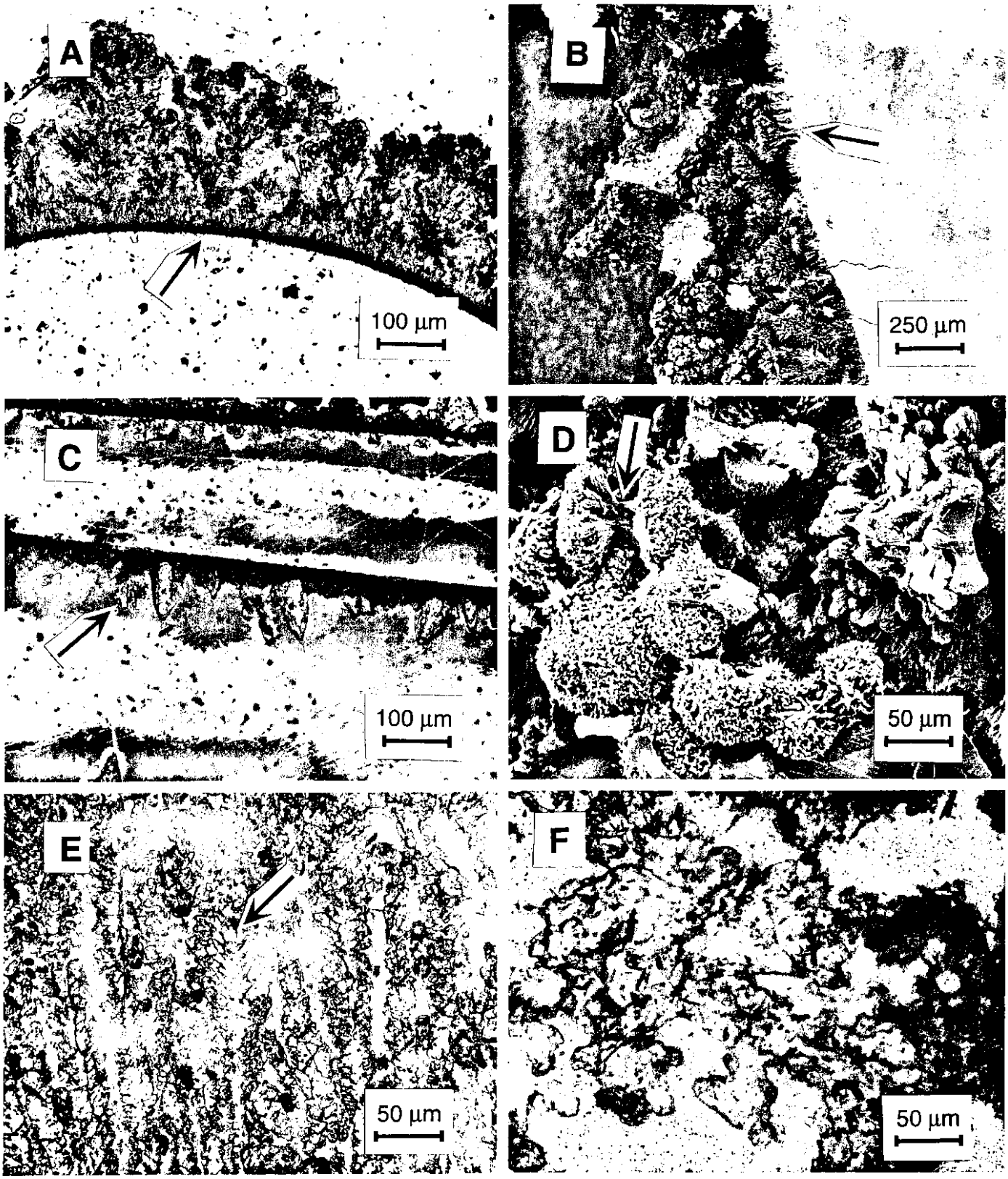

FIG. 9.—Photomicrographs of travertine facies at Angel Terrace Spring AT-1: **A)** microcrystalline calcite wall of a calcified bubble (arrow) from the pond facies encrusted by aragonite needle rims and dendritic shrubs; **B)** SEM micrograph of the same calcified bubble wall shown in Part A; **C)** calcite "ice sheets" from the pond facies, illustrating microcrystalline calcite wall, and underside growth of dendritic aragonite needle shrubs (arrow) and calcite cements; **D)** SEM micrograph of three-dimensional aragonite needle "fuzzy dumbells" (arrow) from same underside of pond facies ice sheet shown in Part C; **E)** calcite feather crystals (arrow) from a microterraecette in the distal-slope facies; and **F)** anhedral calcite crystals and microcrystalline calcite from the distal-slope facies.

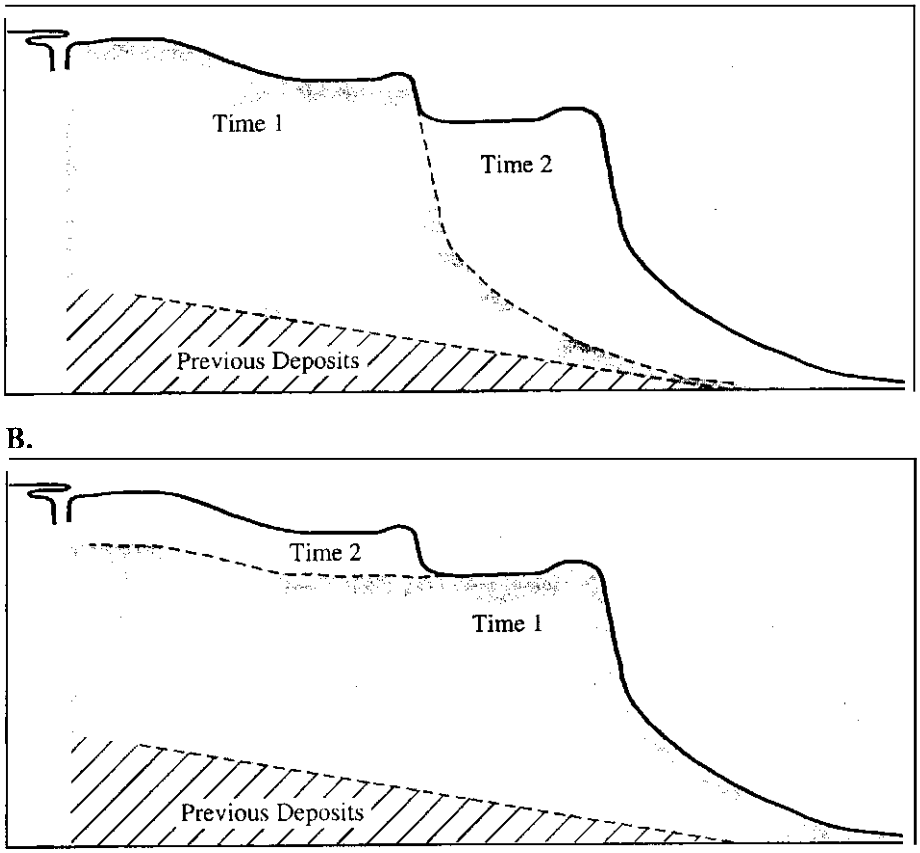

FIG. 10.—Proposed end-member depositional models for travertine formation at Angel Terrace Spring AT-I: A) progradational model: B) backstepping model

Degassing and Evaporation of the Spring Waters at the Surface

The systemstic changes in spring-water isotope geochemistry observed across the Angel Terrace Spring AT-I drainage system (Figs. *6, 7*) suggest that: (I) the large shifts in $\delta^{13}C$ are mainly controlled by rapid degassing of ^{12}C-enriched CO_2 rather than microbial activity and *(2)* the small changes in $\delta^{18}O$ may be caused by evaporation of ^{16}O-enriched water vapor. Spring-water DIC and $\delta^{13}C$ compositions exhibit a strong inverse correlation that is consistent with modeled trajectories for Rayleigh-type fractionation during simultaneous degassing and carbonate precipitation (Fig. 7). The fractionation model of Usdowski et al. (1979) has been used for our model calculation:

$$\ln\frac{Cti}{Ctf} = \left[0.5\left(\frac{1}{\alpha T} + \frac{1}{\alpha T \cdot \alpha S}\right) - 1\right]\cdot \ln\frac{Mti}{Mtf}$$

where $C = n/n+N$, n is the concentration of ^{13}C, and N is the concentration of ^{12}C at the initial (ti) and final (tf) stages of degassing. Because of the low values for n in this type of groundwater system, C is virtually iden-

TABLE 4.—*Isotopic composition of Angel Terrace Spring AT-1 travertine.*

Travertine Sample No	Water Sample No	Lithofacies	Aragonite Calcite	Growth Forms	$\delta^{13}C$ ‰ PDB	$\delta^{18}O$ ‰ SMOW	$^{87}Sr/^{86}Sr$	SO, $\delta^{34}S$ ‰ CUT
970513-1	970519 1A	vent	A	botryoids	2.7	4.0	0.71112	22 9
970513-2		vent	A	botryoids	1.6	4.0		
970513-3		vent	A	botryoids	4.1	4 8		
970513-4	970519.2A	apron a d channel	A	streamers	3.6	5.6		22.6
970513-5	910319.3A	pond	A + C	shrubs	3.1	5.5		22.9
970513-6		pond	A + C	shrubs	4.3	7.3		22 4
970513-7		pond	A + C	shrubs	3.9	6.5		23.8
970513-8		pond	A + C	rafts	4 1	9.3		
970513-9		pond	A + C	bubbles	4 1	8 1		
970513-10		pond	A + C	shrubs	1.1	6.1		21.5
970513-11		pond	A + C	mm terracettes	4.0	6.6		23.1
970513-12	970519.4A	proximal-slope	A + C	scallops	4.2	6.2		22.1
970513-13a	970519 5A	proximal-slope	A + C	microterracettes	4 0	6.g		23.2
970513-13b		proximal-slope	A + C	microterracettes	4 0	7.9		22.6
970513-14	970519-6A	distal-slope	C	spherulites	4.1	8 1	0.71110	24.1
970513-15	970513.7A	distal-slope	C	spherulites	5.2	8.6		22.0

TABLE 5.—*Elemental composition of Angel Terrace Spring AT-1 travertine*

Travertine Sample No.	Water Sample No.	Lithofacies	Ca mg/kg	Mg mg/kg	Mg mol%	Fe mg/kg	Sr mg/kg	Mn mg/kg	Na mg/kg	SO_4 mg/kg	S mg/kg	Ba mg/kg	Ti mg/kg	V mg/kg	P mg/kg
970513-1	970519.1A	vent	384814	54	0	31	2346	23	58	3063	840	35	1	13	100
970513-2		vent	386712	30	0	51	2556	42	69	12231	630	37	3	15	107
970513-3		vent	332127	53	0	8	1865	9	283	3510	1245	46	0	23	85
970513-4	970519.2A	apron and channel	178118	77	0	64	2482	31	159	3532	911	113	3	25	104
970513-5	970519.3A	pond	371238	87	0	31	2561	11	176	2952	1243	65	0	27	87
970513-6		pond	371055	4446	2	47	1481	115	128	8108	4343	80	14	35	90
970513-7		pond								4471					
970513-8		pond	363386	2381	1	55	1762	143	461		1267	124	2	17	84
970513-9		pond	350485	174	0	46	2491	0	580		1764	105	0	14	71
970513-10		pond	170511	107	0	18	2333	3	211	1990	1146	142	3	33	15
970513-11		pond	334463	100	0	74	2317	29	406	5671	1711	245	20	28	82
9790513-12	970519.4A	proximal-slope	111137	0	0	0	2373	0	376	1925	1789	63	0	45	49
970513-13a	970519.5A	proximal-slope	375269	4610	2	116	560	235	362	20628	4663	77	3	0	71
970513-13b		proximal-slope	170729	4848	1	94	619	217	302	19239	5288	17	3	8	103
970513-14	970519-6A	distal-slope	114991	4433	2	52	841	156	489	18873	4816	36	4	15	105
970153-15	970513.7A	distal-slope	165014	4891	2	61	831	130	172	18414	4393	44	0	20	104

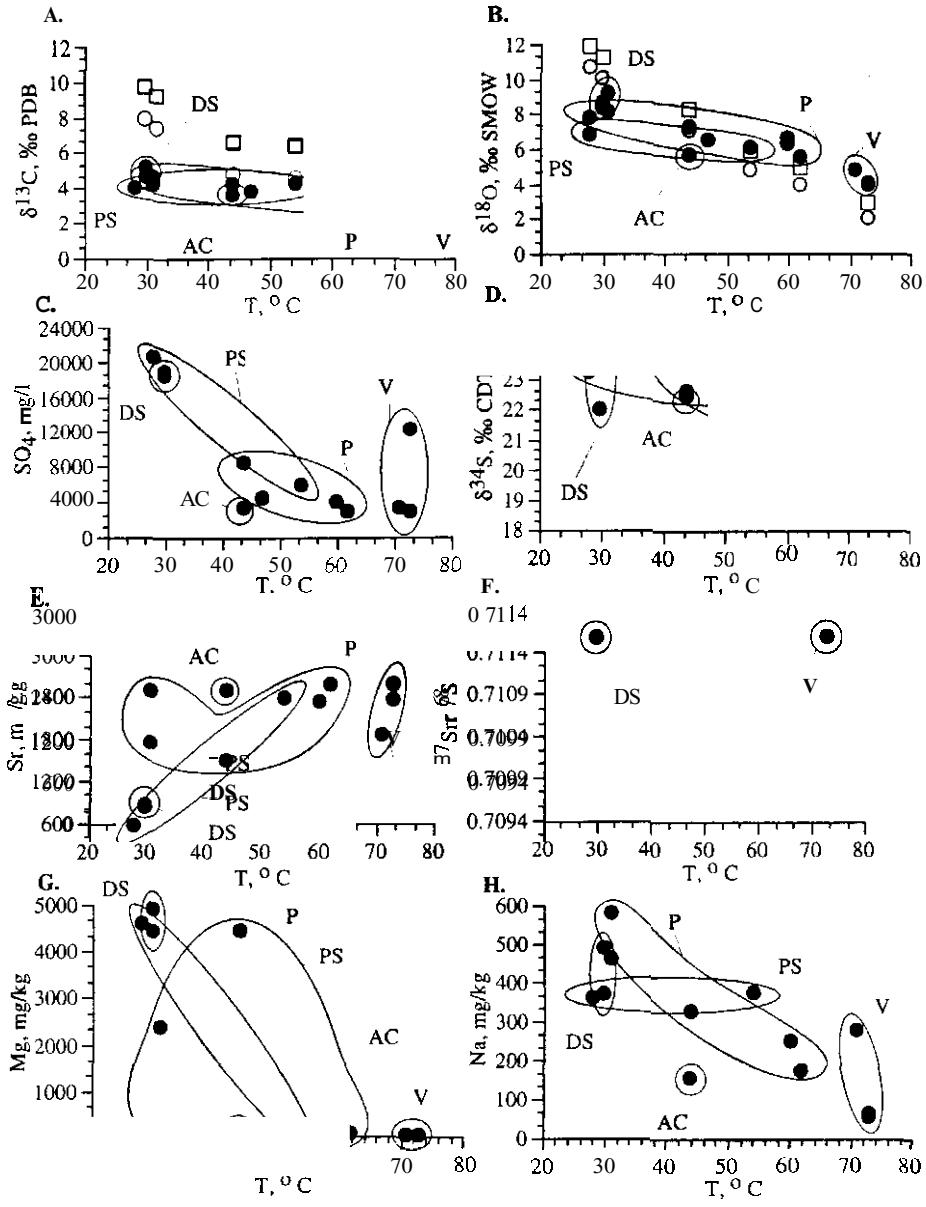

FIG. 11.—Covariation plots of travertine chemistry from Angel Terrace Spring AT-1. Data are presented in Tables 4 and 5. In plots A and B, the open boxes represent predicted isotopic values for aragonite in equilibrium with the spring water, while the open circles are predicted equilibrium values for calcite. Calculations are described in the text. Facies abbreviations are presented in Figure 6.

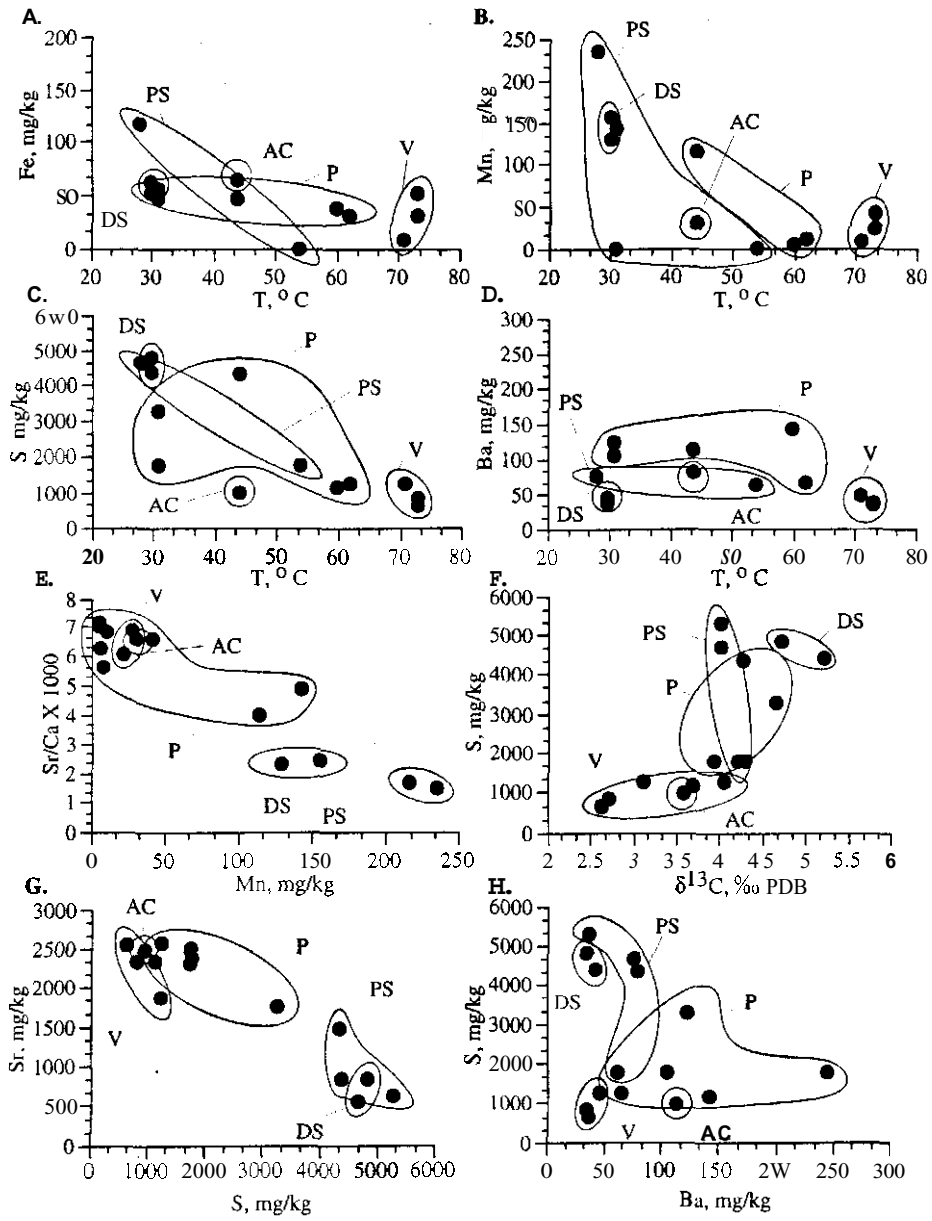

FIG. 12.—*Covariation plots of travertine* geochemistry from **Angel** Terrace Spring **AT-I** Data are presented in Tables 4 and 5. Facies abbreviations are presented in Figure 6.

tical to *n/N,* which is the isotopic ratio R = $^{13}C/^{12}C$. M **is** the total concentration of DIC. The total isotopic fractionation factor (αT) is defined by $\alpha T = (\alpha_f \cdot X, + a_{,,} X_{,,} + a_{,,} . X_{,,})$. The individual fractionation factors (Friedman and O'Neil 1977) are $a_g = C_f/C_g$, $\alpha_b = C_b/C_g$, $a_{,,} = C_d/C_g$ (g = gaseous CO_2, f = dissolved CO_2 + H_2CO_3, b = dissolved HCO_3^-, d = dissolved CO_3^{2-}). The symbul X represents the mole fraction of dissolved carbon. The fractionalion factors α_f, α_b, and $a_{,,}$ were calculated from data in Vogel et al. (*1970*), **Movk** et ill. (*1974*), and Thode et al. (1965). The solid calcite fractionation factur (αS) is defined as C_s/C_g. An estimate of total dissolved CO_2 was calculated using temperature, pH, and DIC (Friedman 1970; Usdowski et al. 1979; Pentecost 1995b; Bethke 1996). Concentrations for CO_2, H_2CO_3, HCO_3^-, and CO_3^{2-} were calculated using temperature-calibrated equilibrium constants (Plummer and Busenberg 1982).

Oxygen-isotope equilibration between atmospheric CO_2, DIC, and H_2O occurs nearly instantaneously. Therefore, little lo no oxygen-isotope fractionation in the water is expected during degassing (Truesdell et al. 1977; Hulston 1977; Panichi and Gonfiantini 1978: Usdowski **et** al. 1979; Tmesdell and Hulston 1986). **A** significant positive shift in water $\delta^{18}O$, however, is expected during evaporation (Lloyd 1966; Gonfiantini 1986). Evaporation of Angel Terrace spring waters is likely given the high temperatures at which the waters emerge, the Iuw humidity of the Yellowstone region, and the large shallow surface area over which the waters spread and How. Application of the equilibrium H_2O liquid--vapor fractionation factors of Horita and Wesolowski (*1994*) suggests that the observed +*1‰* increase in the water (Fig. 6E) would require evaporation of 10 to 15% of the total spring water reservoir as it flows across the drainage system. Conversely. kinetic fractionation would create a much larger effect per volume of evaporated water, yielding a + 1‰ increase in $\delta^{18}O$ with as little as 2% evaporation of the water (Horita and Wesolowski 1994). Although beyond the scope of this pilot study, future analyses of the Angel Terrace spring waters will need to analyze $\delta^{18}O$. δD, and conservative tracers such **as** Cl across the drainage system to conclusively determine the extent of evaporation (Panichi and Gonfiantini 1978; Truesdell and Hulston 1980).

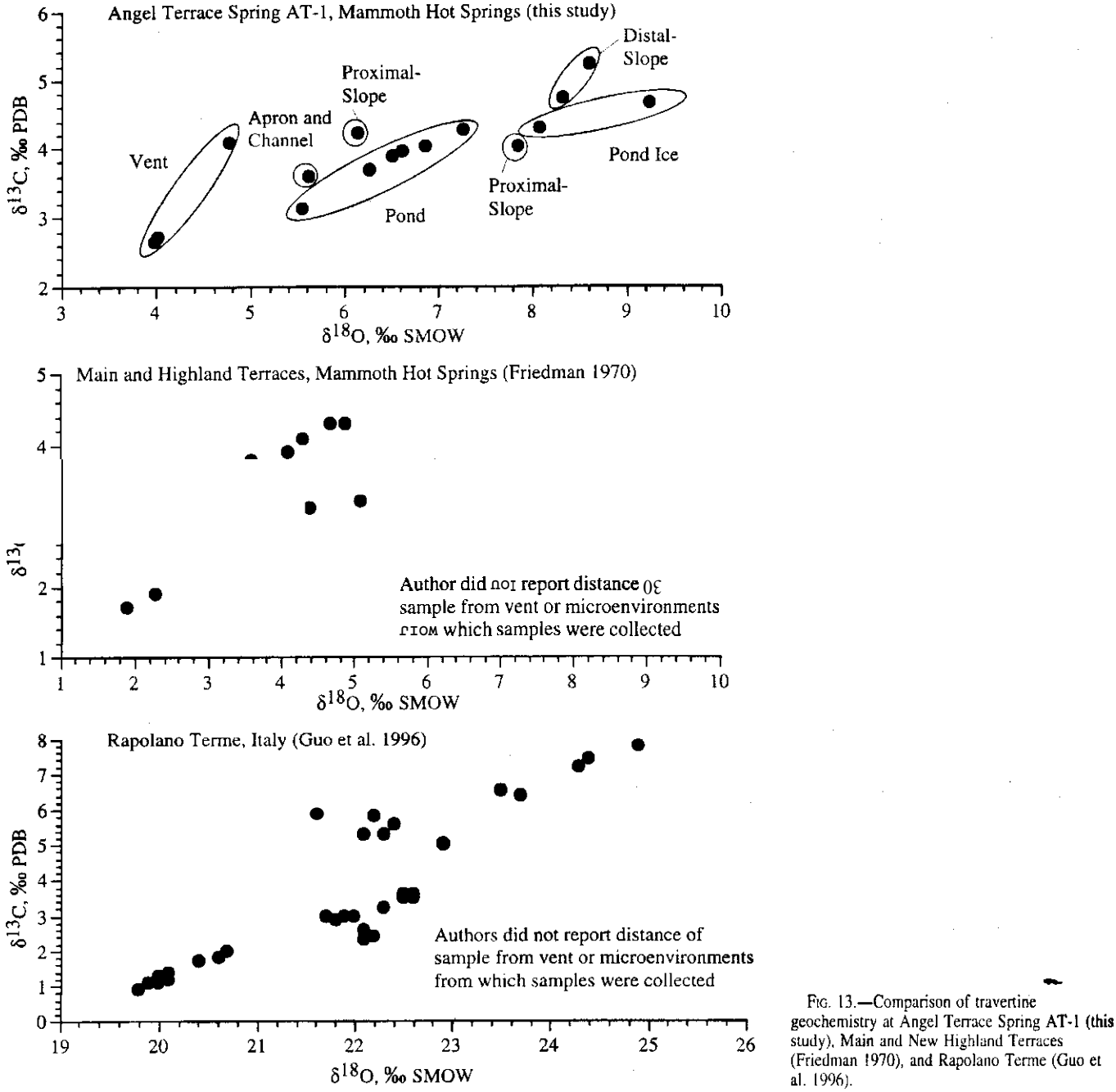

FIG. 13.—Comparison of travertine geochemistry at Angel Terrace Spring AT-1 (this study), Main and New Highland Terraces (Friedman 1970), and Rapolano Terme (Guo et al. 1996).

Processes Controlling Travertine Composition

At temperatures above 44°C aragonite precipitates at Angel Terrace, whereas from 30 to 43°C aragonite and calcite co-precipitate. Below 30°C only calcite precipitates (Fig. 3). These mineralogic changes from aragonite to calcite across the spring system are generally consistent with expected temperature controls on mineralogy (Busenberg and Plummer 1986; Folk 1994). However, the Angel Terrace temperature–mineralogy trends are complicated by two factors. First, the travertine of the higher-temperature pond is composed of mixtures of lower-temperature calcite and aragonite precipitated at the water–air interface (ice sheets, calcified bubbles, aragonite needle aggregates) and higher-temperature aragonite shrubs formed on the pond floors (Table 3). Second, some downstream transport of travertine carbonate crystals takes place, causing mineralogical mixing in the distal parts of the system. In addition, other parameters that vary along the flow path (i.e., water and solid-phase mixing, CO_2 degassing, agitation, ionic strength, rate of precipitation, and temperature) may be influencing travertine mineralogy (Kitano 1962a, 1962b; Lippmann 1973; Folk and Land 1975; Given and Wilkinson 1985; Morse and Mackenzie 1990; Chafetz et al. 1991a; Jones et al. 1996; Renaut and Jones 1996).

A plot of travertine $\delta^{18}O$ versus $\delta^{13}C$ shows a positive covariation trend with a strong linear subset of six analyses in the pond facies (Fig. 13). No appreciable fractionation of either carbon or oxygen isotopes occurs between aragonite and calcite over the temperature range at Angel Terrace (Tarutani et al. 1969; Robinson and Clayton 1969; Romanek et al. 1992; Kim and O'Neil 1997). Therefore, mineralogic changes across the spring system only minimally affect the travertine isotope values. Although dif-

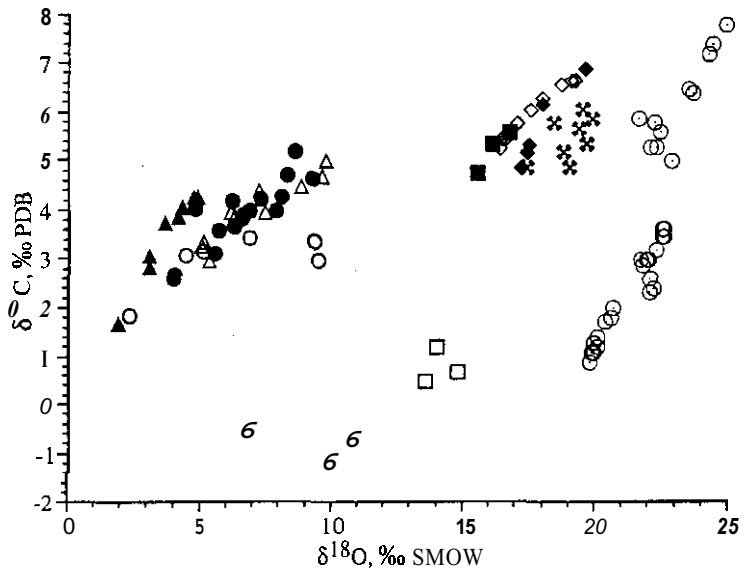

● Angel Terrace. Mammoth Hot Springs, Yellowstone (this study)
O Main **Spring,** Mammoth Hot Springs, Yellowstone (Friedman 1970)
A New Highland Terrace, Mammoth Hot Springs, Yellowstone (Friedman 1970)
△ Narrow Gauge, Mammoth Hot Springs, Yellowstone (Chaietz and Lawrence 1994)
■ Durango, Colorado (Chafetz and Lawrence 1994)
□ Pagosa Springs, Colorado (Chaietz and Lawrence 1994)
✣ Bridgeport, California (Chafetz and Lawrence 1994)
⊙ Rapolano Terme, Siena, Italy (Guo et al. 1996)
✖ La Zitelle Springs, Viterbo, **Italy** (Chafetz and Lawrence 1994)
◆ Bagni San Fillipo, Vitrrho. Italy (Gontiantini et al. 1968)
◇ Bagnaccio, Viterbo. Italy (Gonfiantini et al. 1968)

FIG. 14.—Comparison of travertine geochemistry from several different hot spring localities around the **world.**

ferent in absolute values, the overall carbon and oxygen isotopic trends at Angel Terrace are similar to those observed previously at Mammoth Hot Springs (Friedman 1970), Rapolano Terme, Italy (Guo et al. 1996), and several other sites of hot spring travertine deposition from around the world (Figs. 13, 14). Unfortunately. detailed comparison of the Angel Terrace data with these other studies is not possible because descriptions of the spring microenvironments from which the samples were collected are not reported.

The values of $\delta^{18}O$ versus $\delta^{13}C$ for aragonite and calcite in equilibrium with the spring waters have been calculated for each sampling station (Fig. 11A, B). The minimal fractionation of oxygen and carbon isotopes between aragonite and calcite does not change with temperature or precipitation rate (O'Neil et al. 1969; Grossman and Ku 1986; Romanek 1992; Patterson et al. 1993; Kim and O'Neil 1997), and will therefore not change from the vent to the distal-slope environments. For the oxygen isotopes, equilibrium calcite fractionation was determined using equations presented by Kim and O'Neil (1997), and equilibrium aragonite fractionation was calculated using equations in Grossman and Ku (1986) and Patterson et al. (1993). The dominant dissolved carbonate species shifts from H_2CO_3 to HCO_3^- as the pH increases from 6 to 8 across the Spring AT-I drainage system (Plummer and Busenberg 1982). Therefore, this effect has been corrected by subtracting H_2CO_3–HCO_3^- fractionation as calculated from changing *pH* (Mook et al. 1974) from the total H_2CO_3–$CaCO_3$ fractionation of Romanek et al. (1992).

Both **the** carbon and oxygen isotopic composition of the travertine exhibit slightly elevated, yet near-equilibrium, values relative to the degassed spring waters in the vent, apron and channel, and pond facies (Fig. 11A, B). Conversely, travertine precipitated in the proximal and distal-slope facies exhibit negative shifts of up to −3‰ for both $\delta^{13}C$ and $\delta^{18}O$ with respect to the equilibrium carbonate values (Fig. 11A, B). One possible explanation would be the downstream transport of travertine crystals (originally precipitated in the vent, apron and channel, and pond iacies) intu the proximal and distal-slope facies. Travertine accumulation rates decrease from 30 cm/year in the vent facies to less than 5 cm/year in the distal-slope facies (Fig. 3). **As a** result. small amounts of detrital travertine transported into the distal slope would have **a** disproportionally large isotopic mixing effect. If this is correct, **the** lack of proximal-type crystal fabrics in the distal-slope environment would require that these allochthonous travertine crystals undergo rapid diagenetic alteration to contribute to formation of the blocky calcite *spherules* and possibly the feather calcite crystals (Fig. 9E. F). Equilibrium $\delta^{18}O$ values have been calculated in this study using water data reported from other hot spring localities around the world (Fig. 14). In general, the results illustrate trends strikingly similar to those o b served at Angel Terrace but are difficult to compare directly because of the lack of a precise spatial (proximal-to-distal) context (Fig. 14).

In addition to these transport effects, another factor not evaluated in this study are the potentially large seasonal variations in water temperature **and** chemical composition. especially in late winter and spring during melting of the local snow pack. These melt waters would have lower $\delta^{18}O$ because of meteoric distillation, and potentially lower $\delta^{13}C$ values **as** a result of

accumulating dissolved soil-gas CO_2 derived from local soils (Sorey 1991). Meteoric mixing would also change water temperature and saturation states, creating seasonal variations in crystal growth rates. The magnitude of these seasonal effects in the spring waters and their record in the carbonates will necessarily he an important aspect of future studies at Angel Terrace.

Mineralogy, Solid-Phase Mixing, and Diagenesis

Although the mixed aragonite–calcite mineralogy observed across the Angel Terrace system does not strongly affect hulk isotopic compositions, it may have a significant influence on trace-element compositions. Aragonite and calcite have significantly different equilibrium concentrations and therefore distribution coefficients for Sr, Mg. Na. Mn. and Fe (Veizer 1983; Morse and Bender 1990). As a result, the Angel Terrace travertine trace-element covariations may reflect solid-phase mixing of aragonite and calcite (Figs. 11, 12). This is especially suggested by covariations in Mn abundance versus Sr/Ca (Fig. 12E), which fall along a linear mixing distribution between expected calcite and aragonite end-member compositions.

Travertine $^{87}Sr/^{86}Sr$ ratios are essentially the same in the vent and distal-slope facies (Figs. 5F, 11F), which precludes the use of $^{87}Sr/^{86}Sr$ in tracking detrital transport of carbonates from the vent to the distal slope. Surface meteoric waters contain low Sr abundances (<0.0001 ppm; Sorey 1991) compared to the spring waters (up to 3 ppm; Friedman 1970). Therefore, the spring-water $^{87}Sr/^{86}Sr$ signatures would not detect mixtures of less than 90% surface runoff water (calculated using mixing equalions of Banner and Hanson 1990). The similarity between water and travertine $^{87}Sr/^{86}Sr$ (Fig. 6F, 11F), the decreasing Sr abundances in the travertine (Fig. 11E), and the Mn versus Sr/Ca negative covariations (Fig. 12B) arc suggestive of binary mixing of aragonite and calcite (Veizer 1983; Banner and Hanson 1990). Petrographic evidence of replacement or inversion was only rarely observed (Fig. 8B); obviously altered samples were not chosen for chemical analysis.

Surficial Biotic Processes

While this study emphasizes physical and chemical aspects of the Angel Terrace hot spring system rather than microbiology, dissolved chemical species representing reactants and products of microbial activity have been evaluated (e.g., Berner 1980; Chapelle 1993). Controversy exists over the relative influence of organic versus inorganic controls on the precipitation of travertine aragonite and calcite. One argument favors rapid inorganic degassing of CO, from stream water (Friedman 1970; Pentecost 1995a, 1995b; Guo et al. 1996), and the other suggests biological removal of CO_2 via photosynthesis as a mechanism lor driving precipitation (Amundson and Kelly 1987; Guo et al. 1996). These interpretations of precipitation mechanisms have, however, primarily been made using either water or carbonate chemistry hut nut a systematic analysis of both.

The observed downstream decrease in travertine $\delta^{13}C$ and $\delta^{18}O$ values with respect to calculated equilibrium values (Figs. 7, 15A) may he caused by the geochemical byproducts of photosynthesis and respiration. Photosynthesis preferentially removes $^{12}C^{16}O_2$ from the water. which would serve to elevate the values of $\delta^{13}C$ and $\delta^{18}O$ in the remaining spring water and any carbonates that it precipitates (Lucas and Berry 1985; McConnaughey 1989a, 1989b; Ehleringer et al. 1993; Rau et al. 1997). Because the abundance of photosynthetic microbes increaser downstream, a downstream increase in $\delta^{13}C$ and $\delta^{18}O$ would be expected (Guo et al. 1996). In contrast, travertine isotopic compositions are observed to decrease downstream with respect to calculated equilibrium values (Fig. 11A, Bj. This trend is more consistent with aerobic respiration, which would produce progressively lower 6°C and $\delta^{18}O$ as more CO_2 is released during oxidation of organic matter (Flanagan et al. 1992: Hinga et al. 1994). An additional uncertainty, however, is why the spring-water compositions do not exhibit a downstream temperature-driven decrease in $\delta^{13}C$ with respect to Rnyleigh-type fractionation (Fig. 7) similar to that calculated for the travertine (Fig. 11A). Future studies of the diurnal and seasonal variations in Angel Terrace Spring AT-I water chemistry will be required to fully interpret these isotopic trends.

The H_2S fumes being emitted at Angel Terrace suggest that sulfate reduction is occurring somewhere within the spring system, either in the subsurface plumbing or along the surface outflow. In addition, the high abundance of *Aquificales* bacteria in the vent and apron and channel facies indicates that sulfide oxidization is taking place (Brock 1978). It is currently unknown, however, whether the sulfide is derived from a magmatic source, thermochemical reactions. biological mediation, or subsurface water–rock interactions with limestones, evaporites, or metal sulfides (e.g., Vairavamurthy and Schoonen 1995). As a result. a thorough understanding of the $\delta^{34}S$ and 6°C fractionation in the Angel Terrace system will require future studies of the concentrations, production rates, and isotopic compositions of the dissolved sulfide.

Given these uncertainties. some preliminary hypotheses can he made based on the sulfur data collected thus far. The concentration of sulfate in the Angel Terrace travertine (2900 to 20.700 ppm) is high with respect to Concentrations in aragonites, calcites. and dolomites from other geological settings (Staudt and Schoonen 1995). Sulfate concentrations are approximately 520 ppm in Angel Terrace spring water and about 2700 ppm in seawater (Drever 1988: Lihes 1992). Therefore. Angel Terrace travertine is notably enriched in sulfate relative to marine skeletal carbonates. which have sulfate concentrations in the range of 1000 to 20,000 ppm (Staudt and Schoonen 1995). Spring water and travertine have $\delta^{34}S$ and $^{87}Sr/^{86}Sr$ *signatures* equivalent *to* those of Mississippian seawater (Claypool et al. 1980; Burke et al. 1982; Faure 1986), suggesting that the Angel Terrace spring waters have undergone suhsurface water–rock interaction with limestones and evaporites of the Mississippian Madison Formation (Sorey 1991). Sulfur-isotope compositions of dissolved sulfate in Spring AT-I water are close to +20‰ CDT. with only 1.4‰ variation across the study transect and no systematic change down the Row path. The sulfate $\delta^{34}S$ composition of Angel Terrace travertine (+21.5 and +24.1‰ CDT) is up to 3‰ heavier than the dissolved sulfate (Figs. 6G. 11D) but shows a similar lack of systematic changr down the How path.

These analyses of Angel Terrace spring *water and travertine* $\delta^{34}S$ suggest that redox cycling of sulfur at elevated temperature may play a major role in dictating the environmental conditions and metabolic pathways that dominate the microbial cnmmunity. This assertion is supported by the release of H_2S, which may he in minor concentrations and of inorganic origin, and the abundance of sulfide oxidiring microbes. Despite this direct evidence for both sulfate reduction and sulfide oxidation. the preliminary sulfur-isotope data fail to uniquely delineate the magnitude and character of the metabolic pathways. Specifically, initial $\delta^{34}S$ determinations for carbonate-associated sulfate in travertine samples show little variance from the inferred parent sulfate despite the evidence for redox reactions and associated kinetic isotope effects (Fig. *6)*. The implications are threefold: (1) either the system is sufficiently swamped by sulfate to mask the isotope effects, (2) the rates of microbial reduction and oxidation are lower than predicted from cursory assays of community structure and sulfide concentration, or (3) the isotope effects are offset by a dynamic "steady-state" balance between oxidized and reduced forms.

These results illustrate that the isotopic products of microbial processes are not readily ohserved in the Angel Terrace spring water and travertine sulfur-isotope compositions. The rates and proportions of microhially driven sulfate reduction and sulfide oxidation appear therefore to be insufficient to significantly overprint the large sulfate reservoir of the open spring system. This indicates that while travertinc crystal fabrics are strongly influenced by microbes by providing a substrate for crystal nucleation. the chemical by-products of microbial respiration and photosynthesis are not well expressed in travertine crystal geochemistry

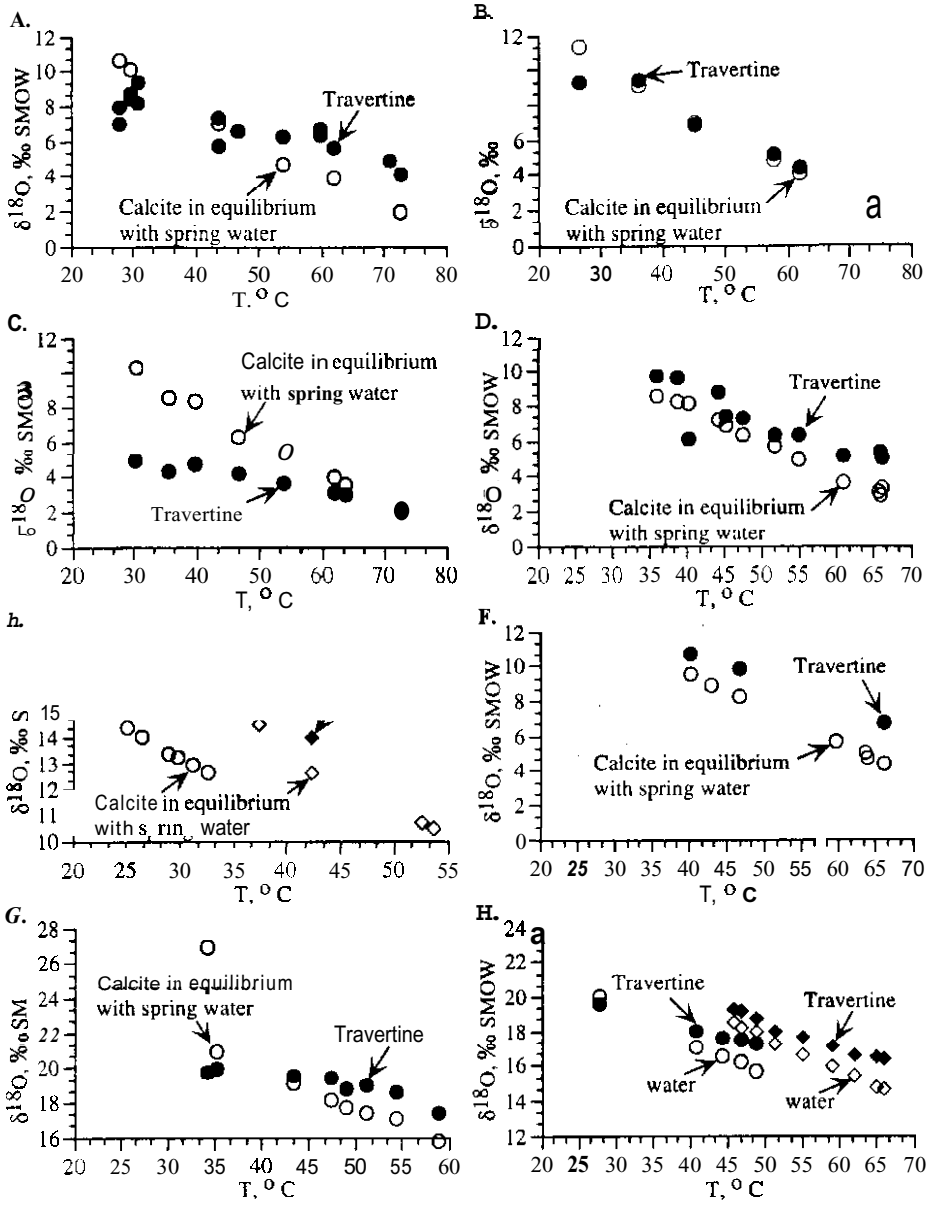

FIG. 15.—Comparison of spring-water and travertine oxygen isotope geochemistry and calculated equilibrium calcite from several different localities around the world: A) Angel Terrace, Mammoth Hot Springs (this study): B) Main Springs, Mammoth Hut Springs (Friedman 1970):C) New Highland Terrace, Mammoth Hut Springs (Friedman 1970); D) Narrow Gauge (Chafetz and Lawrence 19941: E) near Durango (circle symbols) and Pagosa Springs (diamond symbols), Colorado (Chafetz and Lawrence 1994);F) Bridgeport, California (Chafetz and Lawrence 1994); G) La Zitelle, Italy (Chafetz and Lawrence 1994); H) Viterbo, Italy (Gonfiantini et al. 1968).

CONCLUSIONS

Paired spring-water and travertine samples have been systematically analyzed along hydrologic gradients at Angel Terrace, Mammoth Hot Springs, Yellowstone National Park. Results indicate that modern terraced hot spring travertine environments in this area are composed of five depositional facies, which are: (1) vent, (2) apron and channel, (3) pond, (4) proximal-slope, and (5) distal-slope. The travertine in each facies is composed of a distinct assemblage of aragonite needles and calcite crystals organized into characteristic larger-scale carbonate accumulations.

Geochemical evaluation of the chemistry of spring water and underlying travertine suggests that downflow CO_2 degassing, temperature decreases, and possibly evaporation are the primary environmental controls on travertine mineralogy and isotopic compositions. Microbial mats growing on the floor of the spring drainage system serve as passive substrates for travertine precipitation. Active biological control of the chemical composition of the precipitating travertine is generally prevented because of the volumetrically large open-system solute reservoir of the spring-water and the rate at which CO_2 degassing occurs. Exceptions to this are the spring-water and travertine isotopic compositions in the distal depositional facies, which are below values predicted for equilibrium precipitation from the spring waters. This relationship may record aerobic respiration as well as downstream detrital transport of travertine crystals. Therefore, in the case of Angel Terrace travertine, the crystallographic fabrics are generally a better indicator of biological mediation than are associated crystal-chemical compositions (i.e., organic substrates control the general morphology of crystal accumulations). The high degree of spatial and temporal variability within spring systems require that travertine compositions he carefully interpreted in the context of depositional facies models to accurately reconstruct the isotopic and elemental compositions of the parent spring-water.

ACKNOWLEDGMENTS

This work was supported by a University of Illinois Urbana–Champaign Critical Research Initiative grant to B. Fouke, and by a National Research Council grant to B. Fouke awarded on a National Aeronautics and Space Administration Exobiology

Program grant to J. Farmer. We sincerely thank I Wright for conducting oxygen and carbon isotope analyses at the University of Maine, J. Blenkinsop for conducting strontium isotope analyses at Carleton University, J. Donovan for assisting with electron microbe analyses at UC Berkeley, and G. Allion for assistance in conducting sulfate isotopic analyses at Indiana University. Reviews hy T. Lyons. H. Chafetz, A. Pentecost, and J. Grotzinger are gratefully acknowledged for their significant contributions to the content of the manuscript. Discussions with T. Johnson, C. Bethke, T. Anderson, and A. Carozzi were important in developing this study.

REFERENCES

Allen, E.T., and Day, A.L., 1935, Hot Springs of the Yellowstone National Park. Carnegie Institution of Washington, Publication 466, 525 p.

Amundson, R., and Kelly, E., 1987, The chemistry and mineralogy of a CO_2-rich travertine depositing spring in the California Coast Range: Geochimica et Cosmochimica Acta, v. 51, p. 2883–2890.

Banner, J.L., and Hanson, C.N., 1990, Calculation of simultaneous isotopic and trace element variations during rater–rock interaction with application to carbonate diagenesis: Geochimica et Cosmochimica Acta, v. 54, p 3123–3127.

Bargar, K.E., 1978, Geology and thermal history of Mammoth Hot Springs, Yellowstone National Park, Wyoming: U S Geological Survey Bulletin, v. 1444, p. 1–54.

Barnes, I., 1965, Geochemistry of Birch Creek, Inyo County, California: A travertine depositing creek in an arid climate: Geochimica et Cosmochimica Acta, v 29, p. 85–112.

Barnes, I., and O'Neil, J.R., 1971, Calcium-magnesium carbonate solid solutions from Holocene conglomerate cements and travertine in the Coral Range of California: Geochimica et Cosmochimica Acta, v 35, p. 699–718.

Barns, S.M., and Nierzwicki-Bauer, S., 1997, Microbial diversity in modern subsurface, ocean, and surface environments, *in* Banfield, J.F., and Nealson, K.H., eds., Geomicrobiology Interactions Between Microbes and Minerals: Mineralogical Society of America, Reviews in Mineralogy, p 35–71.

Bar-Yosef, O., and Kra, R.S., 1994, Late Quaternary chronology and paleoclimates of the eastern Mediterranean: Radiocarbon: Tucson, Arizona, Radiocarbon, 256 p.

Benson, L., 1994, Carbonate deposition, Pyramid Lake subbasin, Nevada: I. Sequence of formation and elevational distribution of carbonate deposits (tufas): Palaeogeography, Palaeoclimatology, Palaeoecology, v. 109, p 15–87.

Benson, L., White, L.D., and Rye, R., 1996, Carbonate deposition, Pyramid Lake subbasin, Nevada: 4. Comparison of stable isotope values of carbonate deposits (tufas) and the Lahontan lake-level record. Palaeogeography, Palaeoclimatology, Palaeoecology, v. 122, p. 45–76.

Berner, R.A., 1980, Early Diagenesis: A Theoretical Approach: Princeton, New Jersey, Princeton University Press, Princeton Series in Geochemistry, 241 p.

Bethke, C.M., 1996, Geochemical Reaction Modeling, Concepts and Applications New York. Oxford University Press, 397 p.

Bischoff, J.L., Ludwig, K., Garcia, J.F., Carbonell, E., Vaquero, M., Stafford, T.W., Jr., and Jull, A.J.T., 1994, *Dating of the basal Aurignacian sandwich at Abric Romani* (Catalunya, Spain) by radiocarbon and uranium-series: Journal of Archeological Science, v. 21, p. 541–551.

Brock, T.D., 1978, Thermophylic Microorganisms and Life at High Temperatures: New York. Springer-Verlag, 465 p.

Buccino, C., D'Argenio, B., Ferreri, V., Brancaccio, L., Ferreri, M., Panichi, C., and Stanzione, D., 1978, I Travertini della bassa valle del Tanagro (Campania) studio geomorfologio, sedimentologico e geochimico: Società Geologica Italiana, Bollettino, v. 97, p. 617–646.

Buczynski, C., and Chafetz, H.S. 1991, Habit of bacterially induced precipitates of calcium carbonate and the influence of medium viscosity on mineralogy: Journal of Sedimentary Petrology, v 61, p. 226–233.

Burke, W.H., Denison, R.E., Hetherington, E.A., Koepnik, R.B., Nelson, H.F., and Otto, J.B., 1982, Variation of seawater $^{87}Sr/^{86}Sr$ throughout Phanerozoic time: Geology, v 10, p. 516–519.

Busenberg, E., and Plummer, L.N., 1986, A comparative study of the dissolution and crystal growth kinetics of calcite and aragonite, in Mumpton, F.A., ed., U.S. Geological Survey, Bulletin 1578, p. 139–168.

Cabol, R., Cidu, R., Fanfani, L., Zuddas, P., and Zuddas, P.P., 1991, Geochemistry of Funtana Maore travertine (central Sardinia, Italy): Mineralogica et Petrographica Acta, v. 34, p. 77–93.

Chafetz, H.S., Akdim, B., Julia, R., and Reid, A., 1998, Mn- and Fe-rich black travertine shrubs: bacterially (and nannobacterially) induced precipitates: Journal of Sedimentary Research, v. 68, p. 404–412.

Chafetz, H.S., and Buczynski, C., 1992, Bacterially induced lithification of microbial mats: Palaios, v. 7, p 277–293.

Chafetz, H.S., and Folk, R.L., 1984, Travertine: Depositional morphology and the bacterially constructed constituents: Journal of Sedimentary Petrology, v. 54, p. 289–386.

Chafetz, H.S., and Lawrence, J.R., 1994, Stable isotope variability within modern travertine: Géographie Physique et Quaternaire, v. 48, p. 257–273.

Chafetz, H.S., Rush, P.F., and Utech, N.M., 1991a, Microenvironmental controls on mineralogy and habit of CaCO3 precipitates: an example from an active travertine system: Sedimentology, v. 38, p. 107–126.

Chafetz, H.S., Utech, N.M., and Fitzmaurice, S.P., 1991b, Differences in the $\delta^{18}O$ and $\delta^{13}C$ signatures of seasonal laminae comprising travertine stromatolites: Journal of Sedimentary Petrology, v. 61, p. 1015–1028.

Chapelle, F.H., 1993, Ground-Water Microbiology and Geochemistry: New York, John Wiley and Sons, Ltd., 424 p.

Chesterman, C.W., and Kleinhampl, F.J., 1991, Travertine Hot Springs: Mono County California: California Geology, v. 44, p. 171–190.

Cipriani, N., Ercoli, A., Malesani, P., and Vannucci, S., 1977, I travertini di Rapolano Terme (Siena): Società Geologica Italiana, Memorie v. 11, p. 31–46.

Claypool, G.E., Holser, W.T., Kaplan, I.R., Sakai, H., and Zak, I., 1980, The age curves of sulfur and oxygen isotopes in marine sulfate and their mutual interpretation: Chemical Geology, v 28, p. 199–260.

Coplen, T.B., Winograd, I.J., Landwehr, J.M., and Riggs, A.C., 1994, 500,000-year stable carbon isotopic record from Devil's Hole, Nevada: Science, v. 263, p. 361–365.

Craig, H., 1953, The geochemistry of the stable carbon isotopes: Geochimica et Cosmochimica Acta, v. 12, p. 53–92.

Craig, H., 1957, Isotopic standards for carbon and oxygen and correction factors for mass-spectrometric analysis of carbon dioxide: Geochimica et Cosmochimica Acta, v. 6, p. 186–196.

Dandurand, J.L., Gout, R., Hoefs, G., Menschel, G., Schott, J., and Usdowski, E., 1982, Kinetically controlled variations of major components and carbon and oxygen isotopes in a calcite-precipitating spring: Chemical Geology, v. 36, p. 299–315.

Des Marais, D.J., 1978, Variable water temperature trap for the separation of gas mixtures: Analytical Chemistry, v. 48, p. 1651–1652.

Dreybrodt, W., Buhman, D., Michaelis, J., and Usdowski, E., 1992, Geochemically controlled calcite precipitation by CO_2 outgassing: Field measurements of precipitation rates in comparison to theoretical predictions: Chemical Geology, v. 97, p. 285–294.

Drever, J.I., 1988, The Geochemistry of Natural Waters: Prentice Hall, New York, 437 p.

Ehleringer, J.R., Hall, A.E., and Farquhar, G.D., 1993, Stable Isotopes and Plant Carbon–Water Relations: New York, Academic Press, 553 p.

Farmer, J.D., and Des Marais, D.J., 1994a, Exopaleontology and the search for a fossil record on Mars: Lunar and Planetary Science, v. 25, p. 367–368.

Farmer, J.D., and Des Marais, D.J., 1994b, Biological versus inorganic processes in stromatolite morphogenesis: Observations from mineralizing sedimentary systems, *in* Stal, L.J., and Caumette, P., eds., Microbial Mats: Structure, Development, and Environmental Significance: NATO ASI Series in Ecological Sciences, v. G35, Berlin, Springer-Verlag, p. 61–68.

Faure, G., 1986, Principles of Isotope Geology: New York, Wiley, 589 p.

Flanagan, L.B., Brooks, R., Varney, G.T., Berry, S.C., and Ehleringer, J.R., 1996, Carbon isotope discrimination during photosynthesis and the isotope ratio of respired CO_2 in boreal forest ecosystems: Global Biogeochemical Cycles, v. 10, p. 629–640.

Folk, R.L., 1993, SEM imaging of bacteria and nannobacteria in carbonate sediments and rocks: Journal of Sedimentary Petrology, v. 63, p. 990–999.

Folk, R.L., 1994, Interaction between bacteria, nannobacteria, and mineral precipitation in hot springs of central Italy: Géographie Physique et Quaternaire, v. 48, p. 233–246.

Folk, R.L., and Land, L.S., 1975, Mg/Ca ratio and salinity: Two controls over crystallization of dolomite: American Association of Petroleum Geologists, Bulletin, v. 59, p. 60–68.

Folk, R.L., Chafetz, H.S., and Tiezzi, P.A., 1985, Bizarre forms of depositional and diagenetic calcite in hot spring travertine, central Italy, p. 349–369.

Ford, T.D., and Pedley, H.M., 1996, A review of tufa and travertine deposits of the world: Earth-Science Reviews, v. 41, p. 117–175.

Fouke, B.W., Beets, C.J., Meyers, W.J., Hanson, G.N., and Melillo, A.J., 1996, $^{87}Sr/^{86}Sr$ chronostratigraphy and dolomitization history of the Seroe Domi Formation, Curacao (Netherlands Antilles): Facies, v. 35, p. 293–320.

Friedman, I., 1970, Some investigations of the deposition of travertine from hot springs: I. The isotope chemistry of a travertine-depositing spring: Geochimica et Cosmochimica Acta, v. 34, p. 1303–1315.

Friedman, I., and O'Neil, J., 1977, Compilation of stable isotope fractionation factors of geochemical interest:, United States Geological Survey, p. KK1–KK12.

Given, R.K., and Wilkinson, B.H., 1985, Kinetic control of morphology, composition, and mineralogy of abiotic sedimentary carbonates: Journal of Sedimentary Petrology, v. 55, p. 109–119.

Gonfiantini, R., 1986, Environmental Isotopes in Lake Studies, *in* Fritz, P., and Fontes, J.C., eds., Handbook of Environmental Isotope Geology: The Terrestrial Environment Part B: Amsterdam, Elsevier, v. 2, p. 113–168.

Gonfiantini, R., Panichi, C., and Tongiorgi, E., 1968, Isotopic disequilibrium in travertine deposition: Earth and Planetary Science Letters, v. 5, p. 55–58.

Grossman, E.L., and Ku, T.-L., 1986, Oxygen and carbon isotope fractionation in biogenic calcite: Chemical Geology, v. 59, p. 59–74.

Guo, L., and Riding, R., 1992, Aragonite laminae in hot water travertine crusts, Rapolano Terme, Italy: Sedimentology, v. 39.

Guo, L., Andrews, J., Riding, R., Dennis, P., and Dresser, Q., 1996, Possible microbial effects on stable carbon isotopes in hot spring travertine: Journal of Sedimentary Research, v. 66, p. 468–473.

Hayes, J.M., Des Marais, D.J., Peterson, D.W., Schoeller, D.A., and Taylor, S.F., 1977, High precision stable isotope ratios from microgram samples: Advances in Mass Spectrometry, v. 7, p. 475–480.

Herman, J.S., 1994, Karst geomicrobiology and redox chemistry: State of the science: Geomicrobiology Journal, v. 12, p. 137–140.

Herman, J.S., and Lorah, M.M., 1987, CO_2 outgassing and calcite precipitation in Falling Spring Creek, Virginia, U.S.A.: Chemical Geology, v. 62, p. 251–262.

Herman, J.S., and Lorah, M.M., 1988, Calcite precipitation rates in the field: Measurement and prediction for a travertine-depositing spring: Geochimica et Cosmochimica Acta, v. 52, p. 2347–2355.

Hinga, K.R., Arthur, M.A., Pilson, M.E.Q., and Whitaker, D., 1994, Carbon isotope fractionation by marine phytoplankton in culture: the effects of CO_2 concentration, pH, temperature, and species: Global Biogeochemical Cycles, v. 8, p. 91–102.

HORITA, J., AND WESLOWSKI, D.J., 1994. Liquid–vapor fractionation of oxygen and hydrogen isotopes of water from the freezing to critical points' Geochimica et Cosmochimica Acta, v. 58, p. 3425–3437.

HULSTON, J K , 1977. Isotope work applied to geothermal systems at the Institute of Nuclear Sciences, New Zealand: Geothermics, v 5, p. 89–96.

JONES, B., AND RENAUT, R.W.. 1996a, Influence of thermophilic bacteria on calcite and silica precipitation in hot springs with water temperatures above 90°C: Evidence from Kenya and New Zealand: Canadian Journal of Earth Sciences, v 33, p. 77–83.

JONES, B., AND RENAUT, R.W., 1996b, Morphology and growth of aragonite crystals in hot spring travertine at Lake Bogoria, Kenya: Sedimentology, v. 43.

JONES, B.. RENAUT, R.W.. AND ROSEN, M.R., 1996, High temperature (>90°C) calcite precipitation at Waikite Hot Springs, Nonh Island, New Zealand: Geological Society of London Journal, v. 153, p. 481–496

JONES, B., RENAUT, R.W.. AND Rosin, M.R.. 1998. Microbial biofacies in hot spring sinters: A model bared an Ohaaki Pool, Nonh Island. New Zealand: Journal of Sedimentary Research, v 68. p. 413–434.

KHARAKA, Y.K., MARINER, R.H.. BULLEN, T.D., KENNEDY, B.M., AND STURCHIO, N.C., 1991, Geochemical investigations of hydraulic connections between Corwin Springs Known Geothermal Area and adjacent parts of Yellowstone National Park, *in* Sorey, M., ed.. Effects of Potential Geothermal Development in the Corwin Springs Known Geothermal Resources Area. Montana, on the Thermal Features of Yellowstone National Park: U.S. Geological Survey, Water-Resources Investigations Report 91-4052, p F1–F38.

KIM. S.-T., AND O'NEIL, J.R., 1997, Equilibrium and non-equilibrium oxygen isotope effects in synthetic carbonates: Geochimica et Cosmochimica Acta, v. 61, p. 3461–3475

KITANO, Y , 1962a, A study of the polymorphic transformation of calcium carbonate in thermal springs with an emphasis on the effect of temperature: Chemical Society of Japan, Bulletin v. 35. p 1980–1985.

KITANO, Y., 1962b, The behavior of various inorganic ions in the separation of calcium carbonate from a bicarbonate solution: Chemical Society of Japan, Bulletin v. 35, p. 1973–1980.

LIBES, S.M.. 1992, An Introduction to Marine Biogeochemistry: New York. Wiley, 736 p.

LIPPMANN, F. 1973. Sedimentary Carbonate Minerals: Berlin, Springer-Verlag, 228 p.

LLOYD, R.M., 1966, Oxygen isotope enrichment of sea water by evaporation: Geochimica et Cosmochimica Acta, v. 30, p. 801–814.

LOVE, K.M., AND CHAFETZ, H.S.. 1988, Diagenesis of laminated travertine crusts, Arbuckle Mountains, Oklahoma: Journal of Sedimentary Petrology, v. 58, p. 541–445.

LOVE, K.M., AND CHAFETZ. H S.. 1990, Petrology of Quaternary travertine deposits, Arbuckle Mountains, Oklahoma, *in* Herman, J.S., and Hubbard, D.A., eds., Travertine–Marl: Stream deposits in Virginia Charlottesville, Virginia Division of Mineral Resources, p 65–74.

LUCAS, W.J.. AND BERRY, I.A.. 1985, Inorganic Carbon Uptake by Aquatic Photosynthetic Organisms Rockville, Maryland. American Society of Plant Physiologists, 494 p.

LUDWIG, K R., SIMMONS, K.R.. SZABO, B.J., WINOGRAD, I.J., RIGGS, A.C., LANDWEHR, J.M.. AND HOFFMAN, R.J.. IN? Mass-spectrometric ^{230}Th–^{234}U–^{238}U dating of the Devil's Hole calcite vein: Science, ■. 258, p. 284–287

MCCONNAUGHEY, T.. 1989a, $\delta^{13}C$ and $\delta^{18}O$ isotopic disequilibrium in biological carbonates: I. Patterns: Geochimica et Cosmochimica Acta, v. 53, p. 151–162.

MCCONNAUGHEY, T., 1989b, $\delta^{13}C$ and $\delta^{18}O$ isotopic disequilibrium in biological carbonates: II. In vitro simulation of kinetic isotope effects: Geochimica et Cosmochimica Acta, v. 53, p. 163–171

MCKAY, D.S.. GIBSON, E.K., THOMAS-KEPTRA, K.L.. VALI, H , ROMANEK, C.S.. CLEMETT, S.J., CHILLIER, X.D.F.. MAECHLING, C.R., AND ZARE, R.N.. 1996, Search for past life on Mars: possible relic biogenic activity in Martian meteorite ALH84001: Science. v 273, p. 924–930.

MCSWEEN. H.Y.., *la*.. 1997. Evidence for life in a Martian meteorite?, Geological Society of America, GSA Today. v. 7, p. 1–7

MICHAELIS, J., USDOWSKI, E.. AND MENSCHEL, ti.. 1985, Partitioning of ^{13}C and ^{12}C on the degassing of CO_2 and the precipitation of calcite: American Journal of Science, v. 285, p. 318–327.

MOOK, W.G.. BOMMERSON, I C.. AND STAVERMAN, W H., 1974, Carbon isotope fractionation between dissolved bicarbonate and gaseous carbon dioxide Earth and Planetary Science Letters. v 22, p. 169–176.

MORSE, J.W., AND BENDER, M L.. 1990. Partition coefficients in calcite: Examination of factors influencing the validity of experimental results and their application to natural systems: Chemical Geology, v 82, p. 265–277.

MORSE. J W. AND MACKENZIE, F.T., 1990, Geochemistry of Sedimentary Carbonates: Amsterdam, Elsevier, Developments in Sedimentology, v. 48, 705 p.

O'NEIL, J.R., CLAYTON, R.N.. AND MAYEDA, T.K.. 1969, Oxygen isotope fractionation in divalent metal carbonates: Journal of Chemical Physics, v 51, p. 5547–5558.

PACE, N.R., 1997, A molecular view of microbial diversity and the biosphere: Science. v. 276. p. 734–740.

PANICHI, C., AND GONFIANTINI, R., 1978, Environmental isotopes in geothermal studies: Geothermics, v b, p. 143–161.

PATTERSON, W.P., SMITH, G.R., AND LOHMANN, K.C.. 1993. Continental paleothermometry and seasonality using the isotopic composition of aragonitic otoliths of freshwater fishes, *in* Swan. P K.. ed., Climate Change in Continental Isotope Records: Geophysical Monograph Series, v. 78. p. 191–202.

PEALE, A.C.. 1883. Mammoth or While Mountain Hot Spnngr of Gardiner's River. *in* Hayden, F.V , ed., Twelfth Annual Report of the United States Geological Survey of the Territories: Part II Yellowstone National Park Geology—Thermal Springs—Topography: Washington. D.C., p. 71–84.

PEDLEY, H.M.. 1990, Classification and environmental models of coal freshwater tufas: Sedimentary Geology. v. 68. p. 143–154.

PENTECOST, A., 1990, The formation of travertine shrubs: Mammoth Hot Spnngr. Wyoming: Geological Magazine, v. 127. p 159–168.

PENTECOST, A., 1995a, Formation of laminate travertine at Bogno Vignone, Italy: Geomicrobiology Journal. v. 12, p. 239–251.

PENTECOST, A , 1995b, Geochemistry of carbon dioxide in six travertine-depositing waters of Italy Journal of Hydrology, v. 167. p. 263–278.

PENTECOST, A., 1995c, Significance of the biomineralizing microniche in a *Lyngbya* (cyanobacterium) travertine: Geomicrobiology Journal, v 13, p. 213–222.

PENTECOST, A., 1995d, The Quaternary travertine deposits of Europe and Asia Minor: Quaternary Science Reviews, v 14, p. 1005–1028

PENTECOST, A.. AND SPIRO, B., 1990, Stable carbon and oxygen isotope composition of calcites associated with modern freshwater cyanobacteria and algae: Geomicrobiology Journal, v 8, p 17–26.

PENTECOST, A., AND VILES, HA.. 1994, A review and reassessment of travertine classification: Géographie Physique et Quaternaire, v. 48, p. 305–314.

PIERCE, K.L.. ADAMS, K.D.. AND STURCHIO, N.C.. 1991, Geologic setting of the Corwin Springs Known Geothermal Area–Mammoth Hot Spnngr area in and adjacent to Yellowstone, *a* Sorey, M.. ed., Effects of Potential Geothermal Development in the Corwin Spring, Known Geothermal Resources Area, Montana, on the Thermal Features of Yellowstone National Park: U.S Geological Survey. Water-Resources Investigations Report 91-4052, p. C1–C37.

PLUMMER, L.N., AND BUSENBERG, E.. 1982, The solubilities of calcite, aragonite. and vaterite in CO_2–H_2O solutions between 0 and 90°C and an evaluation of the aqueous model for the system $CaCO_3$–CO_2–H_2O: Geochimica et Cosmochimica Acta, v. 46, p. 1011–1040.

POPP, B N.. ANDERSON, T.F., AND SANDBERG, P.A., 1986. Brachiopods as indicators of original isotope composition in some Paleozoic limestones: Geological Society of America, Bulletin v. 56, p. 715–727.

RAU, G.H.. RIESBESELL, U., AND WOLF-GLADROW, D., 1997, CO_{2aq}-dependent photosynthetic ^{13}C fractionation in the ocean: a model versus measurements: Global Biogeochemical Cycles. v. 11, p 267–278.

RENAUT, R W.. AND JONES, B., 19%. Controls on aragonite and calcite precipitation in hot spring travertine at Chemurkeu, Lake Bogoria, Kenya: Canadian Journal of Eanh Science ■. 34, p. 801–818.

ROBINSON, M , AND CLAYTON, R.N , 1969, Carbon-13 fractionation between aragonite and calcite: Geochimica et Cosmochimica Acta, v. 33, p. 997–1032.

ROMANEK, C.S.. GROSSMAN, E.L., AND MORSE, J.W., 1992, Carbon isotope fractionation in synthetic aragonite and calcite: Effects of temperature and precipitation rate: Geochimica et Cosmochimica Acta, v 56. p. 419–430

SANDERS, J E.. AND FRIEDMAN, G.M.. 1967. Origin and occurrence of limestones, *in* Chilinger, G.V.. Bissell, H.J , and Fairbridge, R.W., eds.. Carbonate Rocks: Amsterdam, Elsevier, Developments in Sedimentology, v. 9, 322 p.

SCHWARCZ, H.P.. LIRITZIS, Y.. AND DIXON, A., 1980, Absolute dating of travertines from Petralona Cave. Khalkidiki Peninsula, Greece: Anthropos, v 7. p. 152–73.

SCHWARCZ, H.P., 1997, Uranium series dating, *in* Taylor, RE., and Aitken, M.I.. eds., Chronometric Dating in Archaeology: Advances in Archeological and Museum Science: New Ynrk. Plenum Press, p. 159–182.

SOREY, M.L., 1991, Effects of potential geothermal development in the Corwin Springs known geothermal resources area, Montana, on the thermal features of Yellowstone National Park U.S. Geological Survey, Water-Resources Investigations Report 91-4052, 110 p.

SOREY, M.L., AND COLVARD, E.M.. 1997, Hydrologic investigations in the Mammoth Corridor, Yellowstone National Park and vicinity, U.S.A.: Geothermics, v. 26, p. 221–249.

STAUDT, W.J., AND SCHOONEN, M.A.A.. 1995, Sulfate incorporation into sedimentary carbonates, *in* Vairavamurthy, M.A., and Schoonen, M.A.A., eds., Geochemical Transformations of Sedimentary Sulfur: American Chemical Society, Symposium Series, v. 612, p. 332–345.

STETTER, K.O., 1996, Hyperthermophiles in the history of life, *in* Bock, G.R., and Goode, J.A., eds., Evolution of Hydrothermal Environments on Earth (and Mars?): Chichester, U.K., Wiley, p. 1–10.

STURCHIO, N.C., 1990, Radium isotopes, alkaline earth diagenesis, and age determination of travertine from Mammoth Hot Springs, Wyoming, USA: Applied Geochemistry, v. 5, p. 631–640.

STURCHIO, N.C., MURRELL, M.T., PIERCE, K.L., AND SOREY, M.L., 1992, Yellowstone travertine: U-series ages and isotope ratios (C, O, Sr, U), *in* Kharaka, Y.K., and Maest, K.M. eds., Water–Rock Interaction: Rotterdam, Balkema, p. 1427–1430.

STURCHIO, N.C., PIERCE, K.L., MURRELL, M.T., AND SOREY, M.L., 1994, Uranium-series ages of travertine and timing of the last glaciation in the northern Yellowstone area, Wyoming–Montana: Quaternary Research, v. 41, p. 265–277.

TARUTANI, T., CLAYTON, R.N., AND MAYEDA, T.K., 1969, The effect of polymorphism and magnesium substitution on oxygen fractionation between calcium carbonate and water: Geochimica et Cosmochimica Acta, v. 33, p. 987–996.

THODE, H.G., SHIMA, M., REES, C.E., AND KRISHNAMURTY, K.V., 1965, Carbon-13 isotope effects in systems containing carbon dioxide. bicarbonate. carbonate. and metal cations: Canadian Journal of Chemistry, v 43, p 582–595.

TRUESDELL, AH.. AND HULSTON, J R., 1986. Isotopic evidence on environments of geothermal systems, *in* Fritz, P.. and Fontes, J.C., eds., Handbook of Environmental Isotope Geology: The Terrestrial Environment Pan A: Amsterdam, Elsevier, v 2, p. 179–226.

TRUESDELL, AH.. NATHESON, M.. AND RYE, R.O, 1977. The effects of boiling mid dilution on the isotopic compositions of Yellowstone Thermal Waters: Journal of Geophysical Research, v. 82. p 3694–3703

USDOWSKI, E., HOEFS, J., AND MENSCHEL, G., 1979. Relationship between $\delta^{13}C$ and $\delta^{18}O$ fractionation and changes in major element composition in a recent calcite-depositing spring—a model of chemical variations with inorganic $CaCO_3$ precipitation: Earth and Planetary Science Letters, v 42, p 267–276.

VAIRAVAMURTHY, M.A., AND SCHOONEN, M.A.A., 1995, Geochemical Transformations of Sedimentary Sulfur. American Chemical Society Symposium Series, v. 612, 467 p.

VALLEY, J.W., EILER, J.M., GRAHAM, C.M., GIBSON, E.K., ROMANEK, C.S., AND STOLPER, E.M., 1997, Low-temperature carbonate concretions in the martian meteorite ALH84001: Evidence from stable isotopes and mineralogy: Science, v. 275, p. 6133–1638.

VEIZER, J., 1983, Chemical diagenesis in carbonates: Theory and application of trace element technique. *in* Anhur, M.A., and Anderson, T.J., edr., Stable Isotopes in Sedimentary geology: Society of Economic Paleontologists and Mineralogists Short Course, no. 10, p. 3–100.

VOGEL, I.C., GROOTES, P.M., AND MOOK, W.G., 1970, Isotopic fractionation between gaseous and dissolved carbon dioxide: Zeitschrift der Physik, v. 230.

WALTER, M.R., AND DES MARAIS, D.J., 1993, Preservation of biological information in thermal spring deposits: Developing a strategy for the search fur fossil life on Mars: Icarus, v. 101, p. 129–143.

WHITE, D.E., FOURNIER, R.O., MUFFLER, L.P.I., AND TRUESDELL, A.H., 1975, Physical results of research drilling in thermal areas of Yellowstone National Park, Wyoming: U.S. Geological Survey, Professional Paper 892, 70 p.

WINOGRAD, I.J., COPLEN, T.B., SZABO, B.J., AND RIGGS, A.C., 1988, A 250,000-year climatic record from Great Basin vein calcite: Implications far Milankovitch theory: Science, v. 242, p. 1275–1280.

WINOGRAD, I.J., COPLEN, T.B., LANDWEHR, J.M., RIGGS, A.C., LUDWIG, K.R., SZABO, B.J., KOLESAR, P.T., AND REVESZ, K.M., 1992, Continuous 50,000-year climate record from vein calcite in Devil's Hole, Nevada: Science, v. 258, p. 255–260.

WOESE, C.R., 1987, Bacterial evolution: Microbiology Reviews, v. 51, p. 221–271.

Received 2 November 1998; accepted 17 August 1999.